LUND UNIVERSITY

Radionuclide Production with PET Cyclotrons, Applications and Preclinical Experiments

Siikanen, Jonathan

2015

Link to publication

Citation for published version (APA):
Siikanen, J. (2015). *Radionuclide Production with PET Cyclotrons, Applications and Preclinical Experiments*. [Doctoral Thesis (compilation), Medical Radiation Physics, Lund]. Medical Radiation Physics, Lund University.

Total number of authors:
1

General rights
Unless other specific re-use rights are stated the following general rights apply:
Copyright and moral rights for the publications made accessible in the public portal are retained by the authors and/or other copyright owners and it is a condition of accessing publications that users recognise and abide by the legal requirements associated with these rights.
• Users may download and print one copy of any publication from the public portal for the purpose of private study or research.
• You may not further distribute the material or use it for any profit-making activity or commercial gain
• You may freely distribute the URL identifying the publication in the public portal

Read more about Creative commons licenses: https://creativecommons.org/licenses/

Take down policy
If you believe that this document breaches copyright please contact us providing details, and we will remove access to the work immediately and investigate your claim.

LUND UNIVERSITY

PO Box 117
221 00 Lund
+46 46-222 00 00

Download date: 06. Dec. 2025

Radionuclide Production with PET Cyclotrons

APPLICATIONS AND PRECLINICAL EXPERIMENTS

Jonathan Siikanen

Medical Radiation Physics
Department of Clinical Sciences
Faculty of Science
Lund University
Sweden 2015

Radionuclide Production with PET Cyclotrons

Applications and Preclinical Experiments

LUND
UNIVERSITY

Jonathan Siikanen

DOCTORAL DISSERTATION
by due permission of the Faculty of Science, Lund University, Sweden.

To be presented to the public on the 13th of May 2015 at 9:00 am at
Föreläsningssalen, Nya Strålbehandlingshuset, Klinikgatan 5, Lund

Faculty opponent

Professor emeritus Hans Lundqvist

Uppsala University, Medical Radiation Physics, Uppsala, Sweden

Organization LUND UNIVERSITY	Document name: Thesis
	Date of issue 150416
Author: Jonathan Siikanen	Sponsoring organization

Title and subtitle: Radionuclide Production with PET Cyclotrons - Applications and Preclinical Experiments

Abstract :

Nuclear medicine is based on the radiotracer principle of George de Hevesy and the magic bullet concept by Ehrlich and focuses on the diagnosis, the treatment of diseases and the investigation of normal states within the human body using radiopharmaceuticals. A radiopharmaceutical is an atom or a chemical compound in which one or several atoms are replaced with a radionuclide. Several diagnostic and therapeutic radionuclides like ^{111}In, ^{99m}Tc and ^{131}I originate from nuclear reactors via a generator or direct production. But to produce many of the conventional PET radionuclides like ^{11}C, ^{18}F, ^{13}N, ^{15}O a particle accelerator like a cyclotron is necessary. Also there is a rapid increase of the research based on engineered mAb fragments and nontraditional antibody-like scaffolds. Approved mAbs and their engineered molecules are now entering the pre-clinical and clinical platforms and both areas have opened up a need for new un-conventional radionuclides with suitable physical and chemical properties that can match all the required half-lives and decay properties set by the different molecules. With the growing interest for imaging and therapeutic nuclear medicine the demand for more and different cyclotron produced radionuclides has increased. This is verified by the increased number of cyclotrons operating in the world. In 2005, ~350 cyclotrons were estimated to be operating in those countries monitored by the International Atomic Energy Agency. A later investigation in 2014 concluded that there are currently more than 950 PET cyclotrons. To access a broad variation of radionuclides the accelerator itself should be equipped with different target systems. The overall objective with the work described in this thesis was to increase and extend the medical radionuclide production with special focus in the design of water and solid targets for a MC 17 Scanditronix PET cyclotron. This thesis is based on the development of two targets with two applications and two preclinical experiments related to these targets.

Key words: Radionuclide production, Cyclotron, PET, SPECT, ^{18}F, ^{89}Zr

Classification system and/or index terms (if any)

Supplementary bibliographical information | Language: English

ISBN:978-91-7623-301-6

Recipient's notes | Number of pages 81 | Price

Security classification

I, the undersigned, being the copyright owner of the abstract of the above-mentioned dissertation, hereby grant to all reference sources permission to publish and disseminate the abstract of the above-mentioned dissertation.

Signature 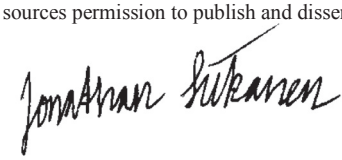 Date 2015-04-07

Radionuclide Production with PET Cyclotrons

Applications and Preclinical Experiments

Jonathan Siikanen

Medical Radiation Physics, Lund University

Department of Clinical Sciences

Lund, Sweden, 2015

LUND
UNIVERSITY

Front cover: A picture of a water holder, made of niobium, in which production of [^{18}F]fluoride takes place by proton bombardment of ^{18}O enriched water.

Thesis for the Degree of Doctor of Philosophy
Faculty of Science at Lund University
Medical Radiation Physics
Department of Clinical Sciences, Lund
Lund University Hospital
Se-221 85 Lund, Sweden

Copyright 2015 © Jonathan Siikanen

Medical Radiation Physics, Department of Clinical Sciences
ISBN: 978-91-7623-301-6 (print)
978-91-7623-302-3 (pdf)

Printed in Sweden by Media-Tryck, Lund University
Lund 2015

”Forward”

Barack Obama and Bruce Springsteen

The day before the presidential election

November 5, 2012, Madison, Wisconsin, USA

Abstract

Nuclear medicine is based on the radiotracer principle of George de Hevesy and the magic bullet concept by Ehrlich and focuses on the diagnosis, the treatment of diseases and the investigation of normal states within the human body using radiopharmaceuticals. A radiopharmaceutical is an atom or a chemical compound in which one or several atoms are replaced with a radionuclide. Several diagnostic and therapeutic radionuclides like ^{111}In, ^{99m}Tc and ^{131}I originate from nuclear reactors via a generator or direct production. But to produce many of the conventional PET radionuclides like ^{11}C, ^{18}F, ^{13}N, ^{15}O a particle accelerator like a cyclotron is necessary. Today there is a rapid increase of the research based on intact monoclonal antibodies (mAbs), engineered mAb fragments and nontraditional antibody-like scaffolds. Approved mAbs and their engineered molecules are now entering the pre-clinical and clinical platforms and both areas have opened up a need for new un-conventional radionuclides with suitable physical and chemical properties that can match all the required half-lives and decay properties set by the different molecules. With the growing interest for imaging and therapeutic nuclear medicine the demand for more and different cyclotron produced radionuclides has increased. This is verified by the increased number of cyclotrons operating in the world. In 2005, ~350 cyclotrons were estimated to be operating in those countries monitored by the International Atomic Energy Agency. A later investigation in 2014 concluded that there are currently more than 950 PET cyclotrons operating in the world. To access a broad variation of radionuclides the accelerator itself should be equipped with different target systems. The overall objective with the work described in this thesis was to increase and extend the medical radionuclide production with special focus in the design of water and solid targets for a MC 17 Scanditronix PET cyclotron. This thesis is based on the development of two targets with two applications and two preclinical experiments related to these targets.

Summary in Swedish

Nuklearmedicin bygger på användning av radioaktiva spårämnen, enligt principen av George de Hevesy, för kartläggning av global och regional funktion hos organ eller patologisk vävnad. Nuklearmedicin inkluderar även användningen av ”Magic bullet”-konceptet enligt Ehrlich där en molekyl används som bärare av radionuklider för att få en radiobiologisk terepeutisk effekt på målvävnanden den riktas mot. Nuklearmedicinska metoder fokuserar på diagnostik och behandling av sjukdomar samt utredningen av normaltillstånd i kroppen med hjälp av radioaktiva läkemedel. Ett radioaktivt läkemedel är en atom eller en molekyl, i vilken en eller flera atomer har ersatts med en radionuklid. Många diagnostiska och terapeutiska radionuklider så som ^{111}In, ^{99m}Tc och ^{131}I produceras i kärnreaktorer och tillhandahålles via en generator eller en direkt produktion. Men för att kunna producera många av de konventionella positron-emitterande (PET) radionukliderna som till exempel ^{11}C, ^{18}F, ^{13}N, ^{15}O behövs någon form av partikelacclerator där en vanlig sådan för medicinsk tillverkning är av typen cyklotron. Idag sker det en kraftig ökning av forskning baserad på intakta antikropppar (mAb) men även på modifierade mAb-fragment vilket har öppnat upp ett behov av nya icke-konventionella radionuklider med nya krav på fysikaliska och kemiska egenskaper. Med det växande intresset för diagnostisk och terapeutisk nuklearmedicin ökar även efterfrågan på fler och olika cyklotronproducerade radionuklider. Detta verifieras av det ökade antalet cyklotroner verksamma i världen. År 2005 uppskattades cirka 350 cyklotroner vara verksamma i de länder som övervakas av Internationella Atomenergiorganet IAEA. En senare undersökning år 2014 visade att det för närvarande finns mer än 950 cyklotroner för medicinsk produktion. För att kunna producera olika radionuklider måste cyklotronerna utrustas med olika strålmålsystem där själva radionuklidproduktionen sker. Det övergripande målet med arbetet som beskrivs i denna avhandling är att öka och utvidga den medicinska radionuklidproduktion med särskild inriktning mot utformningen av vatten och fasta strålmål för en MC 17 Scanditronix PET-cyklotron. Denna avhandling är baserad på utvecklingen av två nya strålmål med två applikationer och två prekliniska experiment associerade till dessa strålmål.

List of papers

This thesis is based on the following papers; which will be referred to in the text by their Roman numerals.

I. A niobium water target for routine production of [^{18}F]fluoride with a MC 17 cyclotron
Siikanen J, Ohlsson T, Medema J, Van-Essen J, Sandell A:
Applied Radiation and Isotopes 72 (2013) 133-136

II. Small scale ^{58}Co production using the neutron flux from a PET cyclotron
Siikanen J and Sandell A: *Manuscript*

III. A solid target system with remote handling of irradiated targets for PET cyclotrons
Siikanen J, Ohlsson T, Tran T.A, Strand S-E and Sandell, A:
Applied Radiation and Isotopes 94 (2014) 294–301

IV. A peristaltic pump driven ^{89}Zr separation module
Siikanen J. Peterson M. Tran, T.A. Roos P. Ohlsson T and Sandell, A:
AIP Conf. Proc. 1509, 206 (2012)

V. Production of ^{89}Zr for biodistribution and dosimetry of ^{89}Zr-trastuzumab in HER2-expressing tumor-bearing nude mice
Fonslet J, **Siikanen J**, Larsson E, Strand S-E, Tran T.A: *Manuscript*

VI. An anesthetic method compatible with ^{18}F-FDG-PET studies in mice
Siikanen J, Sjövall J, Forslid A, Bjurberg M, Brun E, Wennerberg J, Ekblad L, Sandell A: *Accepted for publication in American Journal of Nuclear Medicine and Molecular Imaging, 2015, Article in press*

Reprinted with kind permission from Elsevier (paper I and III) and from AIP Publishing LLC, Copyright [2015] (paper IV)

Preliminary reports

Preliminary reports, not inlcuded in this thesis, have been presented at the following international meetings and conferences

1. Cyclotron produced Ga-66/68 with thermal diffusion-assisted bulk separation and AG50W-X8/UTEVA purification
   Siikanen J, Valdovinos H.F, Hernandez R, Coarasa A.A, McGoron A, Sandell A, Barnhart T.E, Nickles R.J
   Radiometal meeting Sonoma Valley, 2013

2. Production, separation and labeling of ^{45}Ti
   Siikanen J, Hong H, Valdovinos H.F, Hernandez R, Zhang Y, Barnhart T.E, Cai W and Nickles R.J
   SNM annual meeting Vancouver, 2013

3. Labeling proteins with ^{89}Zr separated from large yttrium bulks
   Siikanen J, Ohlsson T, Sandell A, Strand S-E and Tran T.A
   SNM annual meeting San Antonio, USA 2011

4. Using the neutron flux from p,n reactions for n,p reactions on medical cyclotrons
   Siikanen J and Sandell A
   13th Workshop on target and target chemistry, Risö, 2010 Denmark

5. A solid $^{110, 111, 114m}$Indium target with online thermal diffusion activity extraction
   Siikanen J and Sandell A
   13th Workshop on target and target chemistry, Risö, 2010 Denmark

6. Upgrade of a control system for a Scanditronix MC 17 cyclotron
   Siikanen J, Ljunggren K and Sandell A
   13th Workshop on target and target chemistry, Risö, 2010 Denmark

Abbreviations

PET	Positron Emission Tomography
SPECT	Single Photon Emission Tomography
CT	Computer Tomography
MRI	Magnetic Resonance Imaging
BEV	Beam Extraction Valve
^{18}F-FDG	2-[^{18}F]fluoro-2-deoxy-D-glucose
LOR	Line of Response
MR_{glc}	Metabolic Rate of Glucose
SUV	Standardized Uptake Value
mAb	monoclonal Antibody
HER2	Human Epidermal growth factor Receptor 2
PIG	Penning Ion Gauge
RNP	Radionuclidic Purity

Contents

1 Introduction

Nuclear medicine is based on the radiotracer principle of George de Hevesy and the magic bullet concept by Ehrlich (Ehrlich) and focuses on the diagnosis, the treatment of diseases and the investigation of normal states within the human body using radiopharmaceuticals. A radiopharmaceutical is an atom or chemical compound in which one or several atoms are replaced with a radionuclide. For diagnostic purposes the chemical compound or atom is called a radiotracer and it has the purpose to trace and track physiological and biochemical processes in vivo without disturbing the system it was introduced to. Most compounds that are involved in biological processes contain stable ^{12}C, ^{14}N and ^{16}O. By replacing the stable elements in the compounds with radioactive isotopes of the same elements i.e. ^{11}C, ^{13}N and ^{15}O the major functionality of the compound is not changed. For non-ubiquitous elements, i.e. many metals, that normally cannot be introduced directly into a biological compound a chelate is necessary that binds the radionuclide with the compound.

A typical nuclear medicine diagnostic study involves injecting a compound, which is labeled with a photon-emitting radionuclide like ^{99m}Tc or positron-emitting radionuclide like ^{18}F into the body. After injection of the compound the emitted photons from the radionuclides inside the body can be detected in external position sensitive cameras. These cameras are equipped with special detectors that records and follows the radionuclide distribution inside the body as a function of time. In combination with mathematical algorithms the time dependant in vivo radionuclide distribution data can be transformed into functional images.

One of the ground breaking imaging detectors is the scintillation camera or the Anger camera which was introduced in 1958. This type of camera is equipped with a collimator, which only allows detection of perpendicular incoming photons, and it is designed for single photon emitters like ^{99m}Tc and provide planar images of the radioactivity distribution in the body taken from one angle. This image contains little depth information about where the radioactivity is located in this projection. By rotating the camera head and collecting data in several angles around the patient cross sectional images can be reconstructed. This technique is called Single Photon Emission Tomography (SPECT) and acquisition is normally made with two opposite camera heads.

Positron Emission Tomography (PET) utilizes radionuclides which have an excess of protons. These nuclides can either capture an external electron or emit a positive electron i.e. a positron to achieve a more stable nuclear configuration. In the case of positron emission, the positron annihilates with an electron close to the decay site. The electron and positron masses are converted to two almost anti-parallel photons carrying energy of 511 keV. These photons can be detected subsequently in a PET-camera, within a short time window (~ns), defining a line of respons (LOR). From a large number of such lines, the activity distribution can be calculated with mathematical algorithms. Since PET and SPECT techniques results in functional images, they are often combined with anatomically based imaging techniques like Magnetic Resonance Imaging (MRI) or Computed Tomography (CT) to more precisly mark where the functional activity distribution, from PET and SPECT, is located inside the object.

Several diagnostic and therapeutic radionuclides like ^{111}In, ^{99m}Tc and ^{131}I originate from nuclear reactors via a generator or direct production. But to produce many of the PET radionuclides and also some of the SPECT and therapeutic radionuclides, particle accelerators with different energies are necessary. With the growing interest for imaging and therapeutic nuclear medicine the demand for more and different cyclotron produced radionuclides has also increased. This is verified by the increased number of cyclotrons operating in the world. In 2005, ~350 cyclotrons were estimated to be operating in those countries monitored by the International Atomic Energy Agency. A later investigation in 2014 concluded that there are currently more than 950 PET cyclotrons (data is from cyclotron companies: ACSI, GE, IBA, Siemens, Sumitomo; Best etc.) installed around the world (P. Schaffer et al.). To access a broad variation of radionuclides the accelerator itself should be equipped with different target systems.

2 Aims of the thesis

The overall objective with the work described in this thesis was to increase and extend the medical radionuclide production with special focus in the design of water and solid targets for a MC 17 Scanditronix PET cyclotron. This thesis is based on the development of two targets with two applications and two preclinical experiments related to these targets. The papers are referred to their roman numerals in the thesis. First we designed and developed a water target system to optimize and increase the production of [^{18}F]fluoride (paper I). As an application to the water target we investigated the possibilities to use the ejected neutrons originating from (p,n) reactions from routine [^{18}F]fluoride production (paper II) for smale scale radionuclide production. To further increase the possibilities for production of un-conventional radionuclides a solid target system was designed and developed (paper III). The system was tested for production of ^{89}Zr and for this radionuclide we also built an automated separation module (paper IV). To test and use the separated ^{89}Zr we labeled ^{89}Zr to the monoclonal antibody trastuzumab for obtaining biodistribution data in mice (paper V). As a last preclinical experiment we develop a protocol (paper VI) for estimation of metabolic rate of glucose in mice utilizing ^{18}F-FDG. In short the following objectives were met:

I. A niobium water target for routine production of [^{18}F]fluoride with a MC 17 cyclotron.

II. Small scale ^{58}Co production using the neutron flux from a PET cyclotron.

III. A solid target system with remote handling of irradiated targets for PET cyclotrons.

IV. A peristaltic pump driven ^{89}Zr separation module.

V. Production of ^{89}Zr for biodistribution and dosimetry of ^{89}Zr-trastuzumab in HER2-expressing tumor-bearing nude mice.

VI. An anesthetic method compatible with ^{18}F-FDG-PET studies in mice.

3 Nuclear reactions and radionuclide production

3.1 Introduction

In 1901 Wilhelm Conrad Roentgen was awarded the first Nobel Prize in physics for the discovery of the x-ray in November of 1896. In the same time the monumental discovery of the phenomena “radioactivity” by Antoine Henri Becquerel wasn’t given too much attention. However the Nobel Prize in Physics 1903 was divided, one half awarded to Becquerel "in recognition of the extraordinary services he has rendered by his discovery of spontaneous radioactivity", the other half jointly to Pierre Curie and Marie Curie, née Sklodowska "in recognition of the extraordinary services they have rendered by their joint researches on the radiation phenomena discovered by Professor Henri Becquerel". The first artificial radioactivity was created when Irene Joliot-Curie & Frédéric Joliot-Curie bombarded aluminium with alpha particles producing ^{30}P via the ^{27}Al(α,n)^{30}P reaction. After the introduction of the Cockcroft–Walton generator, the cyclotron (Lawrence, 1934; Sloan and Lawrence, 1931) and other types of particle accelerators many elements were bombarded with protons, deuterons, alphas and other types of particles to produce many more new radionuclides.

When the first successful atomic pile chain reactor was constructed in 1942 by a group led by Enrico Fermi another source of manmade radionuclides was made available for the world. In a nuclear reactor, neutrons are produced when uranium or uranium enriched in ^{235}U, ^{233}U or ^{239}Pu undergoes fission and produces heat, fission products and neutrons. Many of the reactor produced radionuclides are induced by the (n.γ) reaction giving rise to important radionuclides like ^{99m}Tc and ^{131}I. The (n.γ) activation route gives, in general “neutron rich” radionuclides which normally decay by the emission of negatively charged β-particles. Neutron capture fission of ^{235}U and ^{239}Pu gives rise to a wide variety of fission products of wich many are of interest as biomedical radionuclides like ^{90}Y and ^{99m}Tc.

In the radioactive ion beam facility ISOLDE at CERN almost the entire periodic table is created simoultaneously by bombarding uranium targets (also they use

other more selectively targets) with high energetic GeV-protons. The produced isotopes are extracted online, from the target, via thermal diffusion. The specific wanted isotope is then selected and collected using a mass separator. ISOLDE is an on-line isotope mass separator facility dedicated to the production of a large variety of radioactive ion beams for many different experiments in the fields of nuclear and atomic physics, solid-state physics, materials science and life sciences.

By having access to an electron accelerator which, generates high intesity bremstrahlung photons, it can be used for high activity production utilizing the (γ,n) reaction. However to be able to chemically separate product from the target material the use of more "low output" reactions like (γ,αn) is more approriate.

Another interesting way to produce radionuclides is to use laser induced reactions. When an intense laser beam interacts with solid targets, beams of megaelectron volt (MeV) protons capable of producing radionuclides are generated. Fritzler *et al* (Fritzler et al., 2003) estimated that MBq-quantities of ^{11}C can be generated using the LOA table-top laser. At JanUSP, using a single pulse at 2×10^{20} Wcm^{-2}, 4.4 kBq of $^{11}C$was generated from a single laser shot. Using a compact laser with similar specifications at 100 Hz after 30 min, this would yield close to 1 GBq of ^{11}C (Ledingham et al., 2004).

In general a nuclear reaction is the reaction between a stable nucleus and a nucleon (i.e. a charged particle or neutron) or a photon which results in the formation of a new nucleus.

3.2 Charged particle activation

Since this thesis is about radionuclide production with PET cyclotrons focus will be on the use of charged particles for radionuclide production. One clear advantage that accelerators possess compared to reactors is the fact that, in general, the target and product are different chemical elements and that the energy of the charged particle beam is variable. This makes it possible to:

Produce high specific activity (SA) preparations, because the target and product are different elements: In radiopharmaceutical terms, specific activity (SA) is the ratio of radioactive tracer to non-radioactive tracer molecules or atoms. High specific activity is required to reach sufficient count level without injecting too high mass. The maximum SA of a radionuclide can be calculated using the equation $SA_{max} = N_A \ln 2/T_{1/2}$, where N_A is Avogadro's number and $T_{1/2}$ is the half-life of the radionuclide. From this equation the theoretical maximum SA for ^{18}F and ^{11}C can be calculated to 6.3 x 10^4 GBq/μmol and 3.4 x 10^5 GBq/μmol

respectively. However, to reach this level no contamination of stable ^{19}F or ^{12}C can be present. This is not the case in practical situations, especially for ^{11}C chemistry. The earth's atmosphere contains about 0.038 % CO_2 and other sources of "cold" carbon contaminations originates from chemistry modules, tubing, target gas and from target irradiation systems.

Separate the product from the target by chemical means: Target masses that are used for irradiation, in a PET cyclotron, normally ranges from a few milligrams to several grams of material. A large production of 100 GBq of ^{18}F inside a one-milliliter water target correspond to an extremely small, in the order of magnitude of 10^{-8}, conversion of original ^{18}O to ^{18}F atoms. To use the different produced radionuclides for further chemistry they need to be separated from the target bulk material. For aqueous targets this can be accomplished by evaporation of the target water or by letting the solution pass through a cat or an ion exchange resin where the radionuclides or the target material is trapped in the resin. Solid targets need to be dissolved into a solution before they are transferred to the resin. Other separation techniques are: solvent extraction, where the entire target is dissolved in a solvent (normally an aqueous solution of either a base or acid) and the radionuclides are extracted with an organic solvent. Thermal diffusion/dry distillation is when a solid target is heated to a temperature where the radioisotopes can be diffused to the surface of the solid target or volatilized from the target material.

Decrease the amount of radionuclidic impurities by selecting the target material, particle and energy window for irradiation: By carefully selecting the target material and (if possible) the charged particle, production of side products can be decreased and thus improve the radionuclide purity (RNP). To minimize unwanted reactions the energy of the bombarding particles can be adjusted to energies below or near threshold for competing reactions and thus improve the radionuclide purity (RNP).

When a charged particle hits a target several processes can occur:

The particles can collide with atomic electrons producing ionizations and excitations of atoms and molecules in the target. The particle slows down and the energy which is lost in the atomic collision is finally transferred to heat. This heat is normally considered problematic and has to be removed with a cooling medium but it can also be useful for separation of produced radionuclides from target material via thermal diffusion.

The particles can collide with the nuclei. The probability of nuclei collision is much smaller than the probability for the collision with atomic electrons. A collision between two particles means that the particles get so close in contact that

a notable interaction between the particles can be observed. Two types of interactions are predominant: strong interaction and electromagnetic interaction.

For nuclear collisions where the incident particle wavelength is large compared to individual nucleons (approximately ≤20 MeV), three types of interactions can occur:

1. Elastic scattering: The kinetic energy is conserved which means that the target stable nucleus remains in its ground state.

2. Inelastic scattering: In this reaction the kinetic energy is not preserved and the stable target nucleus is left in an excited state after the collision. Depending on the level of excitement, i.e. the excitation energy, the nucleus can emit photons or particles to return to its stable state.

3. Absorption: If the bombarding particle is absorbed by the nucleus it leaves the nucleus in a highly excited state. The de-excitation can take place in two ways: by gamma emission or emission of one or more particles.

3.3 Q-value and threshold value

In a nuclear reaction the energy must be conserved, meaning that the combined rest mass and kinetic energy of the reactants must be equal to the combined rest mass and kinetic energy of the products. The Q-value i.e. the net energy between products and reactants may be positive or negative.

Consider the following reaction (fig 3.1):

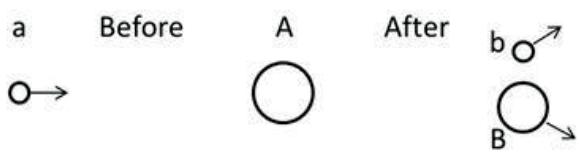

Fig 3.1:
A reaction of an incoming particle, a, with a target atom A yielding the reaction products b and B.

Where a is the accelerated particle, A is the target nucleus, B and b are the reaction products. The reaction is written as:

$a+A \rightarrow B+b$ or $A(a,b)B$

From the relation $E=mc^2$ and the conservation of energy we have:

$$T_a+ T_A+m_ac^2+m_Ac^2=T_b+ T_B+m_bc^2+m_Bc^2$$

Where:
m represents the rest masses

After rearrangement we have

$$m_ac^2+m_Ac^2=m_bc^2+m_Bc^2+T_b+T_B-T_a-T_A$$

The change in kinetic energy is called the reaction Q-value i.e.

$$Q= T_b+T_B-T_a-T_A$$

Hence:

$$m_ac^2+m_Ac^2=m_bc^2+m_Bc^2+Q$$

if $Q>0$ we have an exothermic reaction where mass is converted to energy, energy is released in the reaction.

if $Q<0$ we have an endothermic reaction where kinetic energy is converted to mass, in this case the -Q energy must be brought to the system by the beam.

Threshold value (E_{tr})
When a beam particle of mass m_a strikes the target of nucleus of mass m_A, a part of the momentum is transferred from the particle to the target nucleus. To conserve momentum, an additional kinetic energy of $-q(m_a+m_A)/m_A$ must be added.

If $Q>0$, this implies that the threshold value, E_{tr}, is less than zero, or equals zero from a physical point of view. However, often the projectile and exiting particles are charged and must overcome the Coulomb barrier, $V_{cb,}$ before a reaction can occur. If $V_{cb}>E_{tr}$ then the barrier sets the threshold, which is slightly flexible due to tunneling.

3.4 Reaction cross-section

A nuclear reaction cross section represents the probability that a nuclear reaction will occur through a certain reaction channel like $^{18}O(p,n)^{18}F$. The variation of the cross section as a function of charged particle energy is called an excitation function (fig 3.2). The cross-section is expressed in a "characteristic area" with the unit 'barn'. The cross-section is denoted as σ, and 1 barn=10^{-24} cm^2 which is roughly equal to the geometrical cross-section of an uranium nucleus.

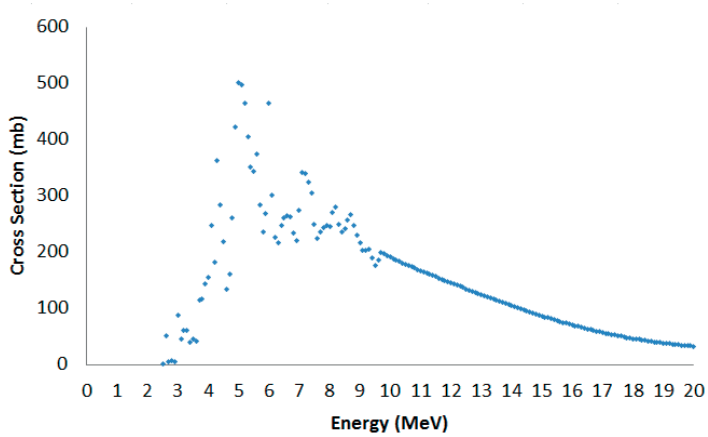

Fig 3.2:
An exctiation function showing the absolute cross sections for the production of ^{18}F via the $^{18}O(p,n)^{18}F$ reaction (IAEA, 2000; Ruth T and Wolf A, 1979)

A cross section can be defined as: If a particle, a, is shot through a surface Y which contains a nucleon A then the probability for the reaction A(a,b)B is equal to σ/Y.

Where:
a = accelerated projectile
A = target
B and b reaction products

As the charged particles continuosly lose kinetic energy when passing through a thick layer of target atoms, the thick target yield is described by:

$$Yield = \frac{3.76 \cdot 10^9}{Z \cdot M} \int_{E_{threshold}}^{E_{max}} \frac{\sigma(E)}{\left(\frac{dE}{dx}\right)} dE(1 - e^{-\lambda t}) \text{ MBq/μA} \qquad \text{eq. 3.1}$$

Where Z is the charge of the incoming particles, M is the mass number of the target atoms, $E_{threshold}$ to E_{max} is the energy window, σ(E) is the cross section at a

certain energy, (dE/dx) is the stopping power in the target, λ is the decay constant and t is the irradiation time. The production yield is here given as MBq/μA from the factor of 3.76×10^9.

From equation 3.1 we see that when irradiation times goes to ∞ the factor $(1 - e^{-\lambda t})$ goes to 1 which corresponds to the saturation value, A_{sat} of the equation $A=A_{sat}(1 - e^{-\lambda t})$. From equation 3.1 we also learn that irradiation times equal to: $1xT_{1/2}=0.5A_{sat}$, $2xT_{1/2}=0.75A_{sat}$, $3xT_{1/2}=0.875A_{sat}$, etc. Radionuclides with shorter half-lives will then of course reach the saturated level faster than long lived radionuclides (fig 3.3). Also from eq 3.1 we understand that it is not production-efficient to bombard targets with irradiation times for much longer than the half-life of the wanted radionuclide.

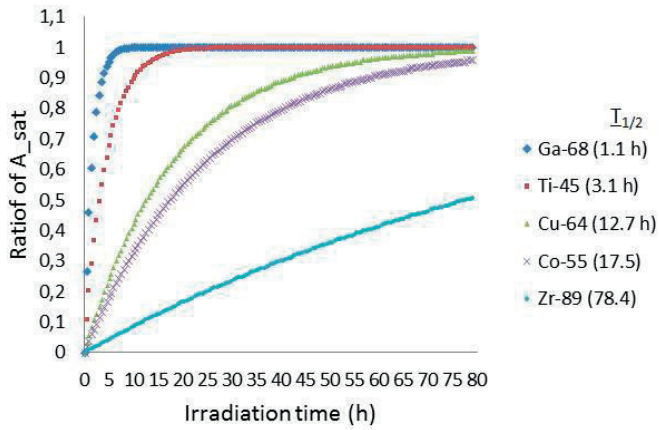

Fig 3.3:
The rise towards maximum activity i.e. saturation activity as a function of irradiation time for different radiometals having half-lives from 1 to 78 hours.

Most clinical PET sites primarily demand radionuclides like ^{18}F for ^{18}F-FDG-production in the morning and then continue with some more short-lived radionuclides such as ^{11}C and ^{13}N. For radionuclides that have longer half-lives, i.e. in the order of days, it can be useful to put beam on these targets whenever there is beam time available. For ^{89}Zr, with a half-life of 78.4 h a 1 GBq-production every day during the week will still result in useful batches for further processing by the end of the week fig 3.4.

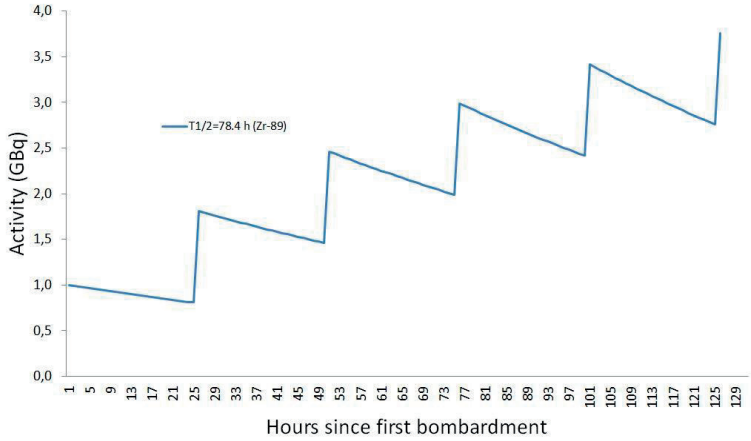

Fig 3.4:
Sequential production of ^{89}Zr ($T_{1/2}$=78.4 h). Owing to the long half-live it can be useful to produce 1 GBq/day over the week and still end up with significant amount of activity by the end of the week despite the decay.

4 PET Cyclotrons in Lund

4.1 Introduction

A common accelerator nowadays is of a cyclic type called a cyclotron. Inside the cyclotron charged particles are created by ionization in the center, accelerated spirally outwards, extracted from the bending magnet force, and directed to a target station. A PET cyclotron, with the primary purpose to create proton rich nuclides, utilizes "proton in and neutron out" (p,n) reactions like $^{18}O(p,n)^{18}F$ or "proton in and alpha out" reactions like $^{14}N(p,\alpha)^{11}C$. A PET cyclotron has typical proton energies between 10-20 MeV with a corresponding beam intensity between 20-150 μA (some machines provide several hundreds of μA). Today the Cyclotron Unit in Lund is equipped with two PET cyclotrons: A Scanditronix MC 17 (17 MeV, 50 μA protons) and a GE PETtrace (16.5 MeV, 130 μA protons).

4.2 Scanditronix MC 17 Cyclotron

The solid and water target systems constructed in this work were mounted and tested on the Scanditronix MC 17 cyclotron in Lund (fig 4.1 and fig 4.2). This cyclotron was the first one from the MC 17 series built by the Swedish company Scanditronix in the late seventies. It was first installed at the Karolinska hospital in Stockholm where it was operated for almost twenty years providing ^{18}F, ^{11}C, ^{13}N and ^{15}O. The cyclotron was then transported to Lund where it was re-installed at Lund University hospital in 2002. Since 2003 the cyclotron has been used for routine clinical production of ^{18}F and it has performed extremely well with only 3 productions cancelled out of 2300 meaning a 99.9 % uptime.

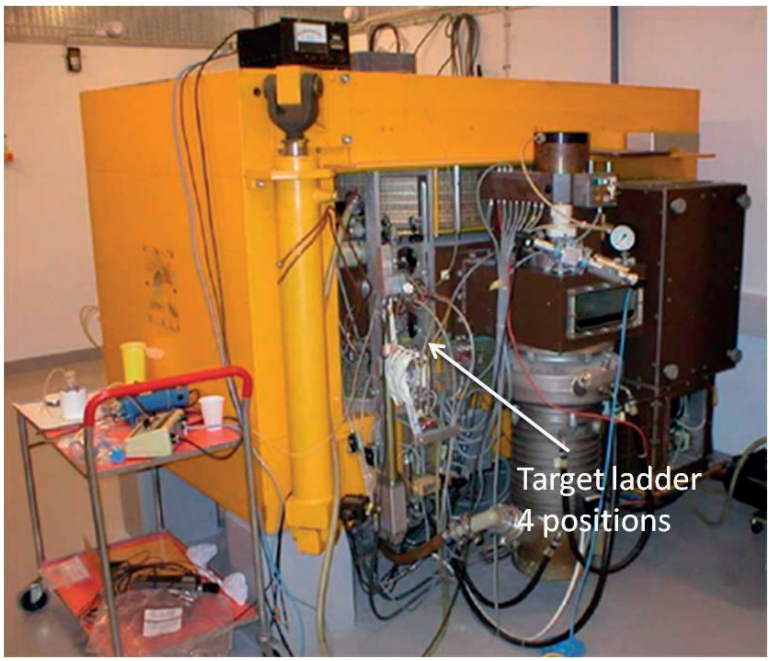

Fig 4.1:
The Scanditronix MC 17 cyclotron installed inside the bunker in Lund. The MC 17 machine is equipped with a target ladder that can hold 4 different targets.

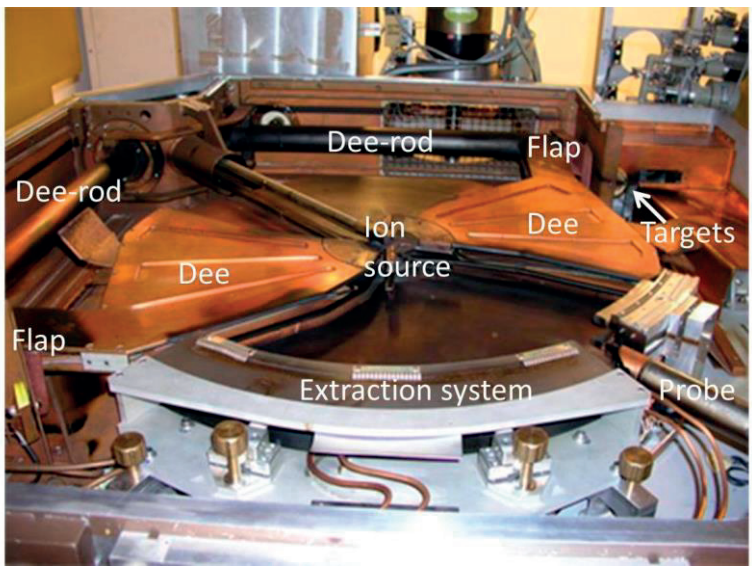

Fig 4.2:
A view of some of the important components inside the Scanditronix MC 17 cyclotron when the upper magnet pole is lifted.

The cyclotron consists of: electromagnet, gradient coils, vacuum pumps, ion source, Radio Frequency (RF)-system, two accelerating hollow electrodes (Dees), power supplies, beam extraction system (negative potential deflector-septum channel combined with harmonic coils), probe (for internal and extracted beam monitoring) and target stations. This cyclotron is a positive-ion proton (p) or deuteron (d) accelerating machine where the charged particles (ions) are created inside a Penning Ion Gauge PIG-source. The PIG-source has two chimneys/tubes with inlets for hydrogen or deuterium gas and slits for outlet of ions (protons and deuterons). On the top and the bottom of the chimney's holes cathodes (tantalum or lanthanum hexaboride) are placed electrically isolated from the chimney (anode). Simultaneously as gas flows through the chimney, voltage (~1000 V) is applied over the cathodes which make them emit electrons. The emitted electrons travels towards the anode in the gas flow. Because of the ion source's orientation in the cyclotron's magnetic main field, the main field will counteract this movement which results in oscillating electrons (they are repelled against the opposite cathode) inside the chimney. When the electrons are oscillating in the gas an ion plasma is created which feeds the cyclotron's puller through the chimney's slit. The RF system extracts the particles, via the puller, from the ion source and accelerates the particles to the final energy in the magnetic field. In Lund the deuteron mode has never been used and focus has been on only protons. Normally 45μA of proton beam is generated from 20 mA ion source current. This corresponds to only 20 W power inside the ion source. To avoid collision with electrons in air, a vacuum of about $3.5*10^{-5}$ mbar is used (gas on) or $1.5*10^{-6}$ mbar (gas off) inside the acceleration chamber.

When a charged particle of mass m and charge q moves with velocity v perpendicularly to a magnetic field B inside a cyclotron, the cyclotron frequency can be derived from the fact that the magnetic Lorentz force $F_m=qvB$ provides the centripetal force $F_c=mv^2/r$: according to figure 4.3. The resulting cyclotron angular frequency, $\omega=qB/m$, is not dependent on the radial position and therefore the circulation time, $T=2\pi m/qB$, is constant at any radius. If an alternating acceleration voltage, with the same frequency as the cyclotron frequency, is applied to the accelerating electrodes (Dees) it means that the timing of the passage for the charged particle over the accelerating gap can be synchronized to the same phase angle of the accelerating sinusoidal potential. This results in an energy increase or energy "kick" of the particles every time the particle passes the accelerating gap. Since the circulation time is constant the particles will have another energy increase as they pass the next acceleration gap. When the energy is increased the radial position is also increased, which results in an outward spiralmovement from center (ion source) as the particles gain energy all the way out to the magnetic peripheral edge.

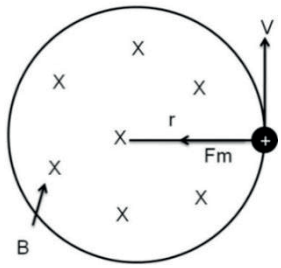

Fig 4.3:
Positively charged particle moving under the influence of a magnetic field force F_m

In MC17 the potential differrence and the actual acceleration is not between the Dees but between the Dees and the ground plane. This results in 4 acceleration steps per lap.

The energy increment per turn, dE/dN, of the particles being accelerated in MC17 is given by the following expression:

$dE/dN=4V_{Dee}\sin(0.5\alpha_{Dee}n)$ eq:4.1

where
V_{dee}=peak acceleration voltage (Dee voltage)
α_{Dee}=angle of the acceleration electrode (Dee angle)
n=harmonic number

Inside the cyclotron the two Dees are supported with two rods. The rods support the Dees, without any contact between the Dee-tips, inside the acceleration chamber. The Dee-rod assembly is an electrical resonator with a combination of capacitance, C, and inductance, L. The inductance corresponds to the circular Dee-rod tubes,while the capacitance arises between the Dee-surfaces and the ground plane. In the MC 17 the two Dee-rod (Dee1 and Dee2) assemblies are inductively connected to each other. In this way the resonance frequency f_0, is split into two resonances, f_{low} & f_{high} (fig 4.4). This creates two modes of operation for the RF: push-push 26.0 MHz (deuterons) and push-pull 26.2 MHz (protons). In push-push mode the phase of the voltage between the two Dees is 0˚ i.e. they are either positive or negative at the same time. In push-pull mode the phase between the dees is 180˚ and they resonate with opposite polarity. The resonance frequency for an electric resonator (LC-circuit) is $f=1/(2\pi(LC)^{1/2})$. To compensate for temperature changes and to keep the resonator at resonance with the RF-feed, the resonance frequency is kept constant by adjustment of 2 flat pieces of metal (part of total C and called flaps (fig 4.2)) that change C by adjusting the distance (motor driven) to the ground plane. The total C sets the resonance frequency and

the difference in C between the two resonators gives the difference in Dee-voltage. This voltage difference is used for centering the beam inside the machine.

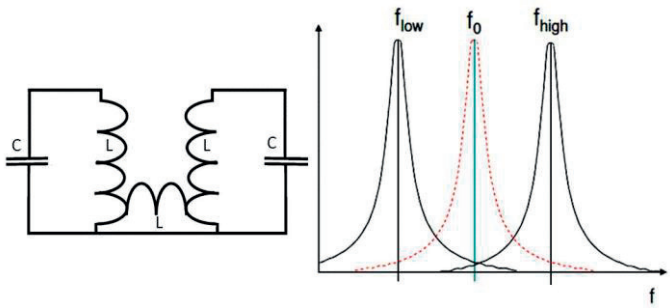

Fig 4.4:
LC-circuit which is used to create two modes of operataion: push-push and push-pull

As the accelerated particles go to higher energies the mass is increased due to relativistic effects. To retain the particles within the cyclotron frequency, $\omega=qB/m$, the magnet field needs to compensate for this relativistic effect with a magnet gradient. In the MC 17 machine this is accomplished with a built in increasing (narrower gap between the poles) mechanical magnetic gradient. Since the gradient needs to be stronger for protons than for deuterons, Scanditronix add an variable electromagnetic component (gradient coils). When the system feeds the coil with a current, I, the gradient fulfills the criteria for deuterons and when fed with current, 2I, it matches the necessary gradient for protons. However in order to get vertical focusing of the beam a negative gradient is nessecary and in the old classic cylotrons it was impossible to have a positive magnet gradient i.e. to compensate for relativistic effects. This resulted in low energy machines that could only acclerate particles up to energies with low relativistic effect. The problem was solved when the magnet poles were cut into sectors giving the nessecary vertical focusing of the beam while maintaining a positive magnet gradient to compensate for relativistic effects.

4.3 MC 17 Beam Profile

To extract the beam, the MC 17 uses a trimming coil-system to introduce a radial oscillation which increases orbit separations and rotates the maximum disturbance to the extraction point. At the extraction point, the charged particles enters a channel with a negative electrostatic deflector (~50 kV) and a grounded septum creating an electric field that pulls out the particles from the bending magnet field. The correlation ratio between the internal beam, before extraction, and the external beam after the deflector is determined with a radially movable probe (fig 4.2). Normal extraction yield is around 75 % during the operation in Lund. The beam

losses, typically 25 %, occur on the septum and other surrounding parts. This constrains the maximum current on targets to about 50 µA. Also the lost current creates activation on certain metal parts which can be problematic during service, and therefore shielding with lead bricks is required. This extraction, where the beam crosses the edge of the main magnetic field almost tangentially, results in horizontal defocusing and a beam profile of (≈35×5 mm^2) as verified from burn mark profiles on havar foils, target foils and beam imaging with aluminum oxide screens (fig 4.5 and 4.6).

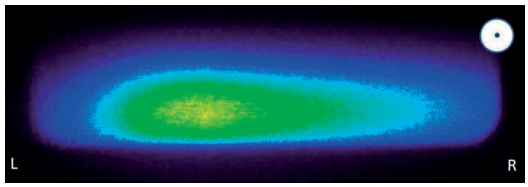

Fig 4.5:
Two dimensional beam profile from the MC 17 cyclotron in Lund. Activation profile is measured from a proton irradiated yttrium foil with an autoradiography system. The autoradiography system (Biomolex 700, Real-Time Digital Imager, Biomolex AS, Norway) used in this set-up detects the emitted particles in a double-sided silicon strip detector (DSSD) (Örbom, 2013).

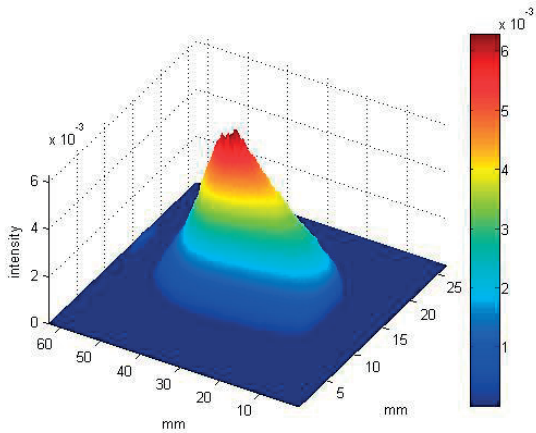

Fig 4.6:
The integrated beamprofile measured using digitalautoradiography of an proton acitvated yttrium foil irradiated with 45 µA protons. Three dimensional representation plotted with matlab from measurement in fig 4.5. The intensity is in an arbitrary unit.

Scanditronix targets are equipped with two-foil He-cooled flanges which physically constrain the beam on the target material to a beam strike area of 10x40 mm^2.

4.4 GE PETtrace cyclotron

The second cyclotron in Lund, which was installed in 2011-2012, is a GE PETtrace (fig 4.7). This machine is also a two particle machine; partly a development of the MC 17, however it accelerates negative ions and uses stripper foils to extract the beam from the bending magnet. When the negatively charged protons or deuterons pass the stripper foil the electrons are removed and the particles change from negative to positive charge, flipping the magnetic bending force from inward to outward. More or less 100 % of the beam is extracted. The beam coming out from the PETtrace is more circular shaped (≈10 mm diameter). The PETtrace is not equipped with trimming-coils and only relies on a mechanical magnetic gradient (decreasing gap between the poles) to compensate for relative mass increase as the particles are accelerated. To handle both proton and deuteron gradients this machine uses the magnet saturation in iron as described earlier (Hagedoorn and Verster, 1963).

Fig 4.7:
The GE PETtrace cyclotron in Lund.

Fig 4.8:
The GE PETtrace beam exiting the cyclotron into atmospheric air (range 25-30 cm) as monitored from the side, after passing 1.25 mm of Al.

5 Targetry

5.1 General overview

Unstable medical radionuclides are obtained by bombarding stable nuclides in the form of solids, gases or liquids, with beams of charged particles. The target materials are held in different target holders i.e. targets. Example schematics of a simple water target and a solid target are depicted in fig 5.1 and fig 5.2.

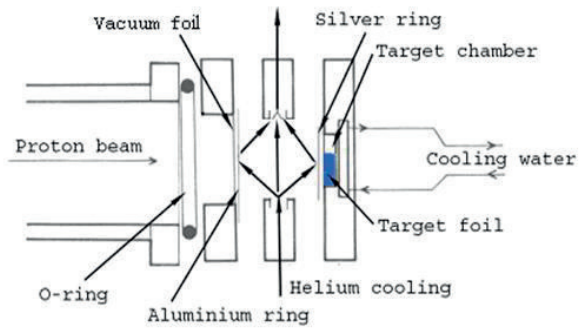

Fig 5.1:
A schematic showing the principle of a water target design

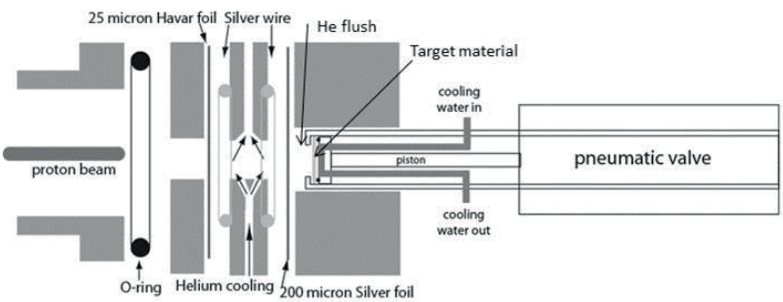

Fig 5.2:
A schematic of a solid target

The water (0.5-10 ml, depending on the design) is contained in a target chamber which is sealed with a thin metal foil (tens of μm). To seal the machine vacuum another thin foil is placed against the beam extraction valve. In between these two foils an inert gas, like He, is re-circulating during irradiation to provide cooling to the foils. To the back side of the target chamber or target backing, normally water is also re-circulating to provide cooling. The same set up is useful for a solid target but here it is not always necessary to contain the target material with a target foil. The charged particles are accelerated in the cyclotron and they pass the foils where they lose some energy before they enter the target material where the wanted radionuclide production takes place. Gas targets are based on the same principle.

5.2 Material properties

There are several of parameters to consider when choosing a suitable material for a new target. Material properties that should be taken into account are:

Thermal conductivity (cooling): The MC17 power input to the target under irradiation is 765 W for a beam intensity of 45 μA (17 MeV · 45 μA). This power must be dissipated away from the target. A material with high heat conduction can more easily transport the heat from the chamber through the targets wall out to surrounding cooling.

Induction of radioisotopes: After an irradiation the target can be activated more or less depending on how much the beam will miss the actual target material and hit the surroundings. It is often necessary to perform adjustments and maintenance on or near the target especially when developing a new target. To avoid unnecessary radiation exposure to personnel it is of high priority to choose a material that is not activated or where the induced activity decays fast.

Chemical resistance of the target backing: The material that holds or contains the target should preferabley be chemically inert, otherwise the target backing will release material ions and other compounds that can obstruct tubing, disturb subsequent chemistry and also decrease specific activity (SA).

In addition to these demands the mechanical strength, the ease of processing-machining the material, and the cost/availability must be considered. It is also an advantage if the material is easily welded.

6 Water target and application

6.1 Introduction

The most important radionuclide in PET is ^{18}F. The reasons why ^{18}F is a suitable positron emitter for PET are many:

- It has a high positron intensity (96.9 % β^+-decay).
- The β^+-energy is low and therefore minimizes its influence on the resulting spatial resolution of the PET camera system.
- It is possible to label different compounds that trace physiological and biochemical processes with ^{18}F since it is useful as a hydrogen substitute. The use of isotopes of the biologically ubiquitous elements makes it possible to label radiopharmaceuticals that trace biochemical processes precisely

Other important radionuclides of ubiquitous elements are presented in table 6.1.

Table 6.1: The "classic" radionuclides used within PET

Radionuclide	$T_{1/2}$ (min)	β^+-yield (%)	E_{max} (MeV)
^{18}F	109.8	96.9	0.64
^{11}C	20.4	99.8	0.96
^{15}O	2.04	99.9	1.72
^{13}N	9.96	100	1.19

There are many ways to produce ^{18}F according to table 6.2. The three most favorable ones are the $^{18}O(p,n)^{18}F$, $H_2{}^{18}O(p,n)^{18}F$ and $^{20}Ne(d,\alpha)^{18}F$ since these reactions only requires moderate particle energies and moderate beam intensities (Guillaume et al., 1991).

Table 6.2: Literature data for the production of ^{18}F for medical use from different nuclear reactions.

Reaction	Target	E (MeV)	Thick target yield[a]	Main form	Reference
$^{18}O(p,n)^{18}F$	$^{18}O_2$	14-0	7.99 GBq/μA[b,c]	$[^{18}F]F_2$	(Ruth T and Wolf A, 1979)
	$^{18}O_2$	10-0	5.55 GBq/μA[c]	$[^{18}F]F_2$	(Nickles et al., 1984)
	$H_2{}^{18}O$	16-0	4.07 GBq/μA[c]	$[^{18}F]F^-$	(Kilbourn et al., 1985)
$^{20}Ne(d,\alpha)^{18}F$	^{20}Ne	14	3.4 GBq/μA[b,c]		(Casella et al., 1980)
	0.1% F_2/Ne	14-2	4.5 GBq/μAh[d]	$[^{18}F]F_2$	(Casella et al., 1980)
	0.18% F_2/Ne	11.2-0	0.37 GBq/μAh	$[^{18}F]F_2$	(Blessing et al., 1986)
	15% H_2/Ne	11.2-0	0.37 GBq/μAh	$[^{18}F]HF$	(Blessing et al., 1986)
	6.7% H_2/Ne	11.2-0	0.30 GBq/μAh	$[^{18}F]F^-$	(Blessing et al., 1986)
$^{20}Ne(d,x)^{18}Ne$[e]	10% H_2/Ne	6.3-0	0.407 GBq/μA[c]	$[^{18}F]HF$	(Robert Dahl et al., 1983)
$^{16}O(\alpha,d)^{18}F$	H_2O	30	0.041 GBq/μAh	$[^{18}F]F^-$	(Clark and Silvester, 1966)
		48	0.259 GBq/μAh	$[^{18}F]F^-$	(Lindner et al., 1973)
$^{16}O(\alpha,2n)^{18}Ne$[e]	O_2	40	0.518 GBq/μAh	$[^{18}F]HF$	(Nozaki et al., 1968)
$^{16}O(^3He,p)^{18}F$	H_2O	41-14	0.259 GBq/μAh	$[^{18}F]F^-$	(Fitschen et al., 1977)
$^{16}O(^3He,n)^{18}Ne$[d]	H_2O	36	0.281 GBq/μAh	$[^{18}F]F^-$	(Knust and Machulla, 1983)
$^{20}Ne(^3He,\alpha n)^{18}Ne$[e]	2% H_2/Ne	27.5	0.19-0.25 GBq/μAh	$[^{18}F]HF$	(Crouzel and Comar, 1978)
		n flux ($cm^{-2}s^{-1}$)	Yield		
$^{16}O(^3H,n)^{18}F$	Li_2CO_3	$3*10^{13}$	7.4 GBq/3h	$[^{18}F]F^-$	(Vera Ruiz, 1988)
	$^6LiOH.H_2O$	$3*10^{13}$	9.25 GBq/3h	$[^{18}F]F^-$	(Vera Ruiz, 1988)

[a]For 1 h experimental irradiation unless otherwise indicated by superscript.

[b]Theoretical yield

[c]Saturation yield

[e]^{18}Ne decays to fluorine-18 with a half-life of 1.67 s

When the PET-camera entered the scene (Phelps et al., 1975), ^{18}F found applications in the nuclear medicine because of its β^+-decay. In the same period of time, the glucose analogue 2-[^{18}F]fluoro-2-deoxy-D-glucose (^{18}F-FDG) was introduced. Before 1986, ^{18}F-FDG could only be synthesized from electrophilic

fluorine, [^{18}F]F_2, produced in gas targets (Fowler et al., 1981; Ido et al., 1978; Shiue et al., 1982). When the Hamacher synthesis (Hamacher et al., 1986) was introduced, ^{18}F-FDG could be manufactured from nucleophilic fluorine i.e.$^{18}F^-$ produced in water targets. With a much better yield (~50 %) it resulted in an increased use of water targets. The advantages of water targets is the ease of handling of the water and the fact that no carrier is needed to extract the ^{18}F as is normally the case for $^{18}F_2$ production. This reults in high specific activty (approximately more than ten times higher than for electrophilic fluorine) when using the $H_2{}^{18}O(p,n)^{18}F$ reaction. Normal oxygen mainly consists of ^{16}O and only 0.2 % ^{18}O. So both ^{18}F reactions, in gas and water, require enriched oxygen and therefore expensive target material.

In the beginning of the development of PET in Lund, [^{18}F]fluoride was produced via the $^{23}Na(\gamma,\alpha n)^{18}F$ reaction utilizing bremsstrahlung photons generated from 100 MeV electrons from the racetrack microtron at the MAX laboratory, Lund. With this set up, a ^{18}F yield of 9.6±0.4 MBq/μAhg sodium was possible (normal sample weights were 5 g) (Ohlsson, 1996). When the production was changed to an electrostatic tandem accelerator (3 MV, Pelletron), using the $H_2{}^{18}O(p,n)^{18}F$ reaction, the productions were increased to a practical yield of 5700±80 MBq (10 μA beam) which was useful in the clinic (Ohlsson et al., 1996).

When the MC 17 cyclotron was brought to Lund in 2002 it came equipped with a water target (Printz and Solin, 1991) which was able to produce around 30 GBq of [^{18}F]fluoride with maximum 22 μA protons for 1 hour irradiation. This irradiation included a refill of 0.6 ml of water after 30 min as the target was irradiated ventilated (which caused a water level decrease due to radiolysis). With higher beam intensities the [^{18}F]fluoride-yield started to drop and the water became discolored similar to Coca Cola (observation in the lab). Back in 2005, the weekly schedule in the Lund cyclotron lab consisted of a production every other Monday for Gothenburg, a production for Växjö and Lund every Thursday and a production for Lund every Friday. To stand prepared for the forthcoming needs and to obtain good margins it was necessary to develop an enhanced target that could utilize the full beam capacity from the MC 17 Scanditronix cyclotron.

6.2 Water target

6.2.1 Water target optimization

The purpose with the work, presented in paper I, was to develop a new and improved target for enriched ^{18}O-water for production of radioactive [^{18}F]fluoride matched to a MC17 Scanditronix cyclotron with a wide proton beam. Earlier water target designs for Scanditronix MC17 (Berridge and Kjellstrom, 1989; Berridge et al., 2002; Medema et al., 2002; Printz and Solin, 1991), are all more or less beam current limited to maximum 30 μA or irradiation time limited. This is because of water thicknesses not optimized to the experimental proton range, excessively small collimators, poor target material or open target chambers. The old target made of silver (Printz and Solin, 1991) provided the facility in Lund with [^{18}F]fluoride for the first two years. The cyclotron has the capacity to deliver beam currents up to 50 μA. However the risk associated with high intensity in a small and thin water volume is that the beam misses the water molecules because of boiling bubbles and cavitation (Steinbach et al., 1990) i.e. the nominal thickness becomes too thin. To avoid this, the target must be constructed in a way so that the experimental thickness will compensate for bubbles and cavitation.

Furthermore the old target is irradiated ventilated. When enriched ^{18}O-water is irradiated, production of oxygen and hydrogen gas will start due to radiolysis (Steinbach et al., 1990). The produced gases can then escape from the chamber through the ventilation which results in a water level that successively decreases. With a closed target this can be avoided. As a result of the open system, bars are used to counteract the He-cooling pressure against the water chamber in the old silver target. A closed target will have an outwards bending due to the higher pressure inside the chamber and therefore the bars which "steal" beam intensity will become unnecessary.

Another disadvantage with the old silver target is the formation of silver colloids during the irradiation process. The colloids give a lower yield of ^{18}F-FDG and obstructions in valves and tubing (Zeisler et al., 2000). A new material that is more chemically resistant and that can tolerate higher intensities is desireable.

Another possible improvement for the old target was to replace the thick silver foils (200 μm), which degrade the proton beam energy down to approximately 13 MeV. The output from the water target increases proportionally to the yield curve for the ^{18}O(p,n)^{18}F reaction in gas when the energy is increased (fig 6.1). The foils should be kept as thin as possible to minimize the energy degradation. The minimum threshold value for the vacuum foil thickness is decided from the strain

of the He-cooling pressure against the cyclotron vacuum. The threshold value for the target foil will be decided from the pressure inside the water chamber.

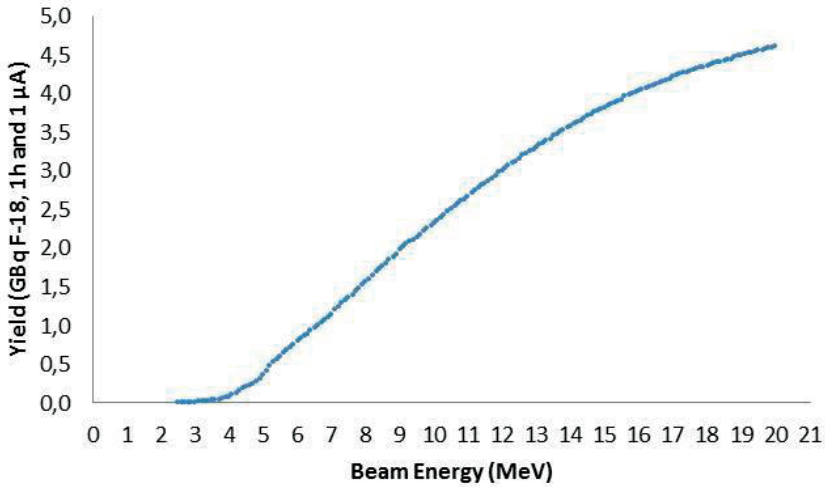

Fig 6.1:
Yield of ^{18}F as a function of beam energy (IAEA, 2000) via the $^{18}O(p,n)^{18}F$ reaction

As a conclusion the identified drawbacks with the old target are:

- The material (silver) is not optimal because the chemical inertness is low and therefore it releases silver colloids that reduce the reactivity of ^{18}[F]fluoride and also obstruct transfer lines (which then requires maintenance and cleaning).
- The water layer is too thin.
- Open system which leads to refills with enriched water during longer production runs.
- Support bars that "steels" intensity from the beam.
- High energy degradation due to 200 µm thick target foil (silver).

Reading the literature resulted in an extra interest for titanium and especially niobium as potential material for the target body. Descriptions of titanium and niobium targets have been presented earlier (Berridge et al., 2002; Schmitz et al., 2002; Zeisler et al., 2000). The benefit with titanium and niobium, compared to

silver, is the chemical resistance, while the drawback is the poor thermal conductivity and higher activation (especially true for titanium). The time course of the exposure outside an irradiated Nb body was investigated by a group at IBA (Schmitz et al., 2002) and it reaches approximately background levels 14 hours after end of bombardment. The exposure originates from the isotope ^{93m}Mo ($T_{1/2}$=6.9 hours). With the relatively short half-life, maintenance close to the niobium target is possible as short as one night after irradiation. The induced activity in the titanium material consists mostly of ^{48}Va with a half-life of approximately 16 days. This will result in a worse build-up of the exposure rate which in the case in the IBA lab reached > 10 mSv/h after approximately four weeks (30 cm from the target body). From a radiation safety point of view the niobium material is better than the titanium material. Physical and mechanical characteristics of niobium, titanium and silver are presented in table 6.3 and 6.4.

Table 6.3: Physical properties of Nb, Ag and Ti

Physical properties	Melting point [°C]	σ at 0-100 °C [$wm^{-1}k^{-1}$]	Density [g/cm^3]	Atomic number
Niobium	2468	53.7	8.57	41
Silver	961.9	429	10.5	47
Titanium	1660	21.9	4.5	22

Table 6.4: Mechanical properties of Nb, Ag and Ti *hard niobium and soft niobium

Mechanical properties	Tensile strength [MPa]	Yield strength [MPa]	Tensile modulus [GPa]
Niobium	585, 330*	550, 240*	104.9
Silver	330	-	82.7
Titanium	230-460	140-250	120.2

6.2.2 Target design

Our first target body was made from a niobium piece (Edstraco AB) 50 mm diameter and 6 mm thick which was later changed to 60 mm diameter and 10 mm thick (fig 6.2). A water chamber of 9 mL, with sloped lower edges for improving the water recovery was milled with a custom made support. The poor heat conductivity of niobium which is about eight times smaller than that for silver according to table 6.3 was compensated by minimizing the thickness of the back wall against the cooling water (0.5 mm).

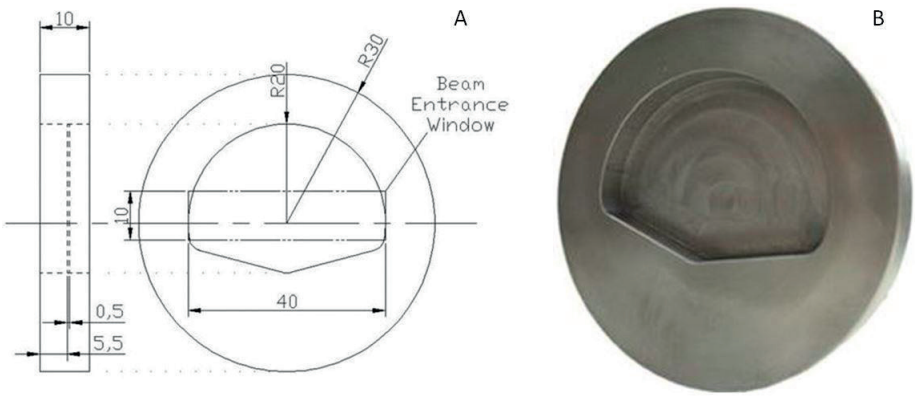

Fig 6.2:
The dimensions of the Nb-disk (A) and the machined Nb-disk (B) used for the water target. The key-hole design is to improve recovery of enriched water which is transferred in and out from the bottom of the disk.

The water level was matched to the beam entrance window with a glass cover in front of the water chamber. A volume of 3.5-4 mL was deemed necessary to cover the beam strike area. Before mounting of the Nb-insert the target needed to be cleaned after the milling procedure. This was done by putting the entire target into aqua regia (nitric acid and hydrochloric acid 1:3 mixture) and letting it boil for about one hour. The aqua regia successfully cleaned the target without any effect on the Nb-material from the harsh aqua regia treatment. The Nb-insert was then mounted in an Al-flange (fig 6.3). Tubes for enriched water transfer were connected with PEEK (poly-etheretherketone) fittings.

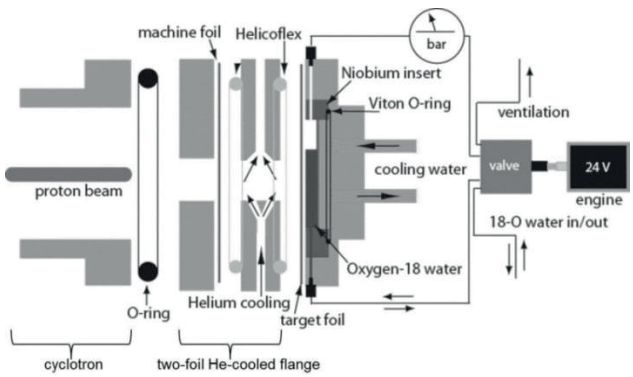

Fig 6.3:
A detailed schematic of the water target

As the machine foil a standard of 25 μm Havar was used. For the target foil, target foil pressure tolerances were calculated with ‘‘Mechanical safety subcommittee

guideline for design of thin windows for vacuum vessels (held not fixed) '' (Western, 1991). A 50 μm Havar foil with a tolerance of around 13 bars was used. The optimal material foil would be to use Nb with the short half-life of the activation product ^{93m}Mo ($T_{1/2}$=6.9 hours) but the calculated pressure tolerances were deemed too low for use in this application (table 6.5). The irradiation of havar, which is an alloy of Co 42.5% / Cr 19.5% / Ni 12.7% / W 2.8 % / Mo 2.6% / Mn and 1.6% / Fe, results in high activation (Manickam et al., 2009) with the potential to cause exposure to personnel.

Table 6.5: Calculated pressure tolerances

Material	Thickness (μm)	Tolerance (Bar)
Nb	100	6
Nb	150	9
Havar	25	6.5
Havar	50	13

To control the valve for filling and emptying the water, a 24 VDC electric engine was used. In the closed looped between target and valve a mechanical pressure meter was mounted to monitor pressure against beam current.

6.2.3 Target performance

The target system (fig 6.4) has worked extremely well and has provided the southern part of Sweden (Lund, Malmö, Göteborg and Växjö) with [^{18}F]fluoride on a daily basis since its installation 2006. The target design has also had a national-international impact with installations on MC 17 cyclotrons in Uppsala (modified to circular beam), Groningen, Toronto, Taipei, St Petersburg and Copenhagen (MC 32, modified to circular beam).

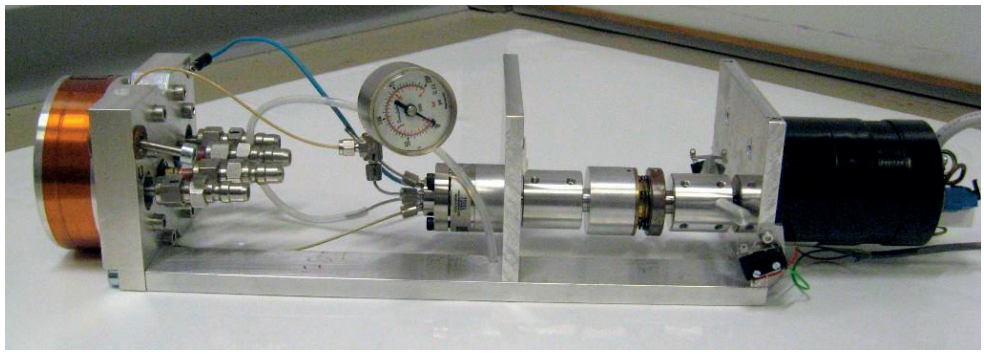

Fig 6.4:
Picture of the water target devloped in Lund. The Nb-water target has two-foil He-cooled flanges and connections for cooling water and He. The opening and closing of the valve is controlled, remotely, with an electric engine.

The first irradiations on the "Lund-target" resulted in a high pressure (≈9 bars) inside the target. This was probably due to beam-degassing of small amounts of debris, rubbish and liquids originating from the new foils and Nb-walls. However after approximatley three runs the pressure started to stabilize to around 4 bars with 45 μA proton irradiation (fig 6.5).

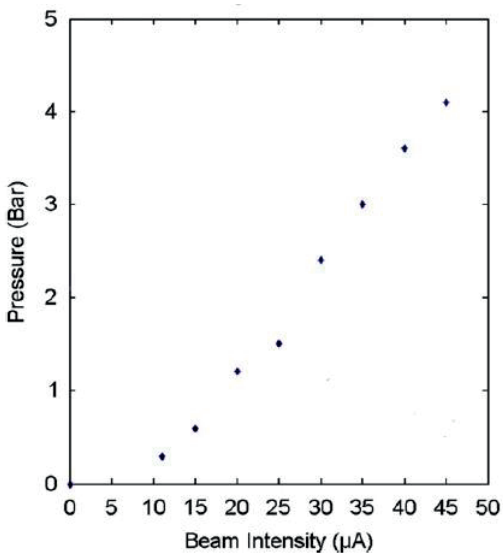

Fig 6.5:
Water target pressure in Lund as a function of beam current

The ^{18}F-yield from low intensity irradiations (5 μA) was compared to the yield from higher intensity (45 μA) as verification if the water layer compensated for boiling bubbles and cavitation. The ^{18}F productions from the low intensity

irradiations (5μA) were only slightly higher (3.6 %) than the high intensity (45 μA) productions thus indicating a well optimized practical proton range thickness of the new Nb-target body. The depth of the Nb-water chamber is 5.5 mm which is approximately twice the thickness compared to the projected range for 15.5 MeV-protons (2.7 mm). The output from the target is more than 110 GBq [^{18}F]fluoride for 1 h irradiation with 45 μA protons. The saturation yield is 8.0±0.6 GBq/μA (n=307). The ^{18}F-FDG yield is 60±5 % and more than 100 GBq ^{18}F-FDG is routinely produced with 2 h, 45 μA protons.

One of the major improvements was the change of target body material. Thanks to the chemical inertness of niobium the beam power did not cause any deterioration of the target body (fig 6.6). The high reactivity and the good quality of the fluoride made in the niobium targets was verified by making ^{18}F-FDG (Hamacher et al., 1986) with TracerLab MX synthesis boxes from G.E.Healthcare.

Fig 6.6:
The old silver target (left picture) with support bars clearly suffers from silver colloid problems originating from the deterioration of the silver because of the proton beam power. The first Nb-body (right picture) was intact even after 8 months of daily productions

6.3 Using the neutron flux from (p,n) reactions for (n,p) reactions

James Chadwick discovered the neutron in 1932. Neutrons are generated during radioactive chain reactions in nuclear power reactors and they can be classified based on their energies. There is no clear boundary between the categories but the following can be used as a guideline (K. Linga and Indrajit, 2012):

Cold neutrons (<0.003 eV)
slow (thermal) neutrons (0.003–0.4 eV)
slow (epithermal) neutrons (0.4–100 eV)
intermediate neutrons (100 eV–200 keV)
fast neutrons (200 keV–10 MeV)
high-energy (relativistic) neutrons (>10 MeV)

There are currently approximately 440 nuclear reactors in the world (K. Linga and Indrajit, 2012). With the report of more than 950 small PET-cyclotrons currently operating (P. Schaffer et al.) this means that the number of PET cyclotrons out number research reactors by more than a factor of two. Charged particle irradiation of a dedicated solid Be-target, in a PET-cyclotron, is a relatively easy way to access fast neutrons via the $^{9}Be(p,pn)^{8}Be$ reaction. The irradiation of a thick beryllium target with tens of μA of 11 MeV protons from a PET cyclotron give rise to a rather intense (~ 10^{11} n/cm^{2}s) source of fast neutrons at the target center (Nickles et al., 1997). This gives a cyclotron facility a very convenient access to an occasional neutron source that can easily be switch on and off. Instead of using a dedicated Be-target it is possible to use already existing neutron fluxes from routine production targets (Bosko, 2005; Bosko et al., 2004). Most PET-cyclotron units around the world have daily production of ^{18}F with several hours of beam on target and therefore also several hours of neutron flux available for "free" during this time because of the ejected fast neutrons originating from the $H_2{}^{18}O(p,n)^{18}F$ reaction. This neutron flux offers a possibility for a parasitic or hitchhiking production of useful isotopes, via neutron activation, by placing target material in the vicinity of the water targets.

The aim of the work presented in paper II was to investigate the possibilities for small scale production of ^{58}Co using the emitted neutrons from a PET-cyclotron. For this purpose natural nickel foils (68.1% ^{58}Ni) were placed behind the [^{18}F]fluoride water target (fig 6.6) (paper I) to produce ^{58}Co ($T_{1/2}$=70.86 d, β+=14.9%, Eγ=811 keV, 99.4%) through the $^{58}Ni(n,p)\,^{58}Co^{m,g}$ reaction. The co-produced metastable state $^{58}Co^{m}$ has a half-life of 9.01 hours and therefore quantification of the ^{58}Co was made after more than five days post bombardment. Furthermore we wanted to use the neutrons to activate thin nickel

wires and use them as ^{58}Co line sources for determination of the spatial resolution performance of a high resolution autoradiography system (Örbom, 2013).

The lower limit of the neutron flux can be calculated using the experimental saturation yield for the water target. For A_sat=8 GBq/μA and a beam intensity of 45 μA this will generate a neutron flux in the target with an order of magnitude of $\approx 10^{11}$ n/s. This only estimates the neutron flux that originates from the (p,n) reaction on ^{18}O all other (p,xn) reaction channels available in the beams path towards and inside the target will also add up to the total neutron flux. To determine the total flux the use of Monte Carlo (Bosko, 2005; Bosko et al., 2004) simulations can be employed or the flux can be measured with for example indium wires (fast neutrons) and manganese wires (thermal neutrons) placed around the target. With the given neutron flux produced from a 45 μA, 17 MeV proton beam it was possible to produce 0.1-0.15 kBq/μAh of ^{58}Co in 0.25 mm thick Ni-foils and 1-1.3 kBq/μAh ^{58}Co in 2 mm thick Ni-foils. The estimated neutron flux on the foils, assuming an isotropic neutron emission, was estimated to approximately 10^{10} $ns^{-1}cm^{-2}$. As a comparison this flux corresponds to the lower end of neutron fluxes produced in a research reactor which has typical neutron fluxes of 10^{10}-10^{14} $ncm^{-2}s^{-1}$. For power nuclear reactors the neutron fluxes can be in the order of 10^{19} $ncm^{-2}s^{-1}$.

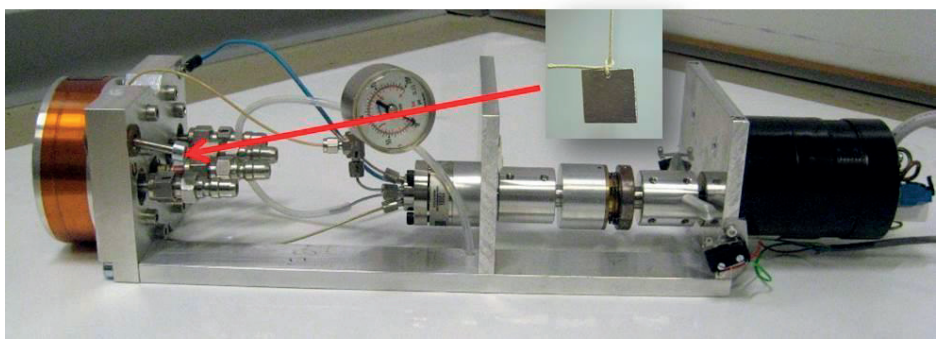

Fig 6.6:
Nickel target materiel is placed behind the water target with a simple wire.

7 Solid target and application

7.1 Introduction

There is a rapid increase of the research based on engineered mAb fragments and nontraditional antibody-like scaffolds but still most of the mAb candidates evaluated in past and ongoing clinical trials are full-length mAbs (van Dongen and Vosjan, 2010). Regardless, approved mAbs and their engineered molecules are now entering the pre-clinical and clinical platforms and both areas have opened up a need for new un-conventional radionuclides with suitable physical and chemical properties that can match all the required half-lives and decay properties set by the different molecules.

Several un-conventional radionuclides useful for PET/SPECT/Therapy can be found in the literature (Holland et al., 2010; Pagani et al., 1997) and some of the most interesting radionuclides, producable with a PET-cyclotron, are summarized in table 7.1. Normally the access of ^{68}Ga is governed by the use of a generator through the decay of ^{68}Ge. An alternative route to generator produced ^{68}Ga is to use charged particle activation of zinc (Engle et al., 2012; Siikanen et al., 2013; Tolmachev and Lundqvist, 1996). The ^{68}Ga generators are widely available and easy to use. However availability of a cyclotron and the limited activity output of commercial generators ($\leq$ 2.8 GBq) motivate direct production. Also for ^{66}Ga no generator is available. All of the listed radionuclides in table 7.1 can be produced by bombardment of target materials in a solid state and therefore they necessitate that the cyclotron is equipped with a solid target system.

Table 7.1: Some radionuclides useful for PET/SPECT/Therapy which can be produced with cyclotrons. Only gammas with intensities >10 % are listed

Isotope	Production Route	$T_{1/2}$	% betas	Mean energy β^+ or β^- (keV)	Eγ:keV (intensity)
^{89}Zr	^{89}Y(p,n)^{89}Zr	78.41 h	22.74 β^+	395.5	909.2 (0.99)
^{124}I	^{124}Te(p,n)^{124}I	100.2 h	22.7 β^+	687.0 & 974.7	602.7 (0.629)
					722.8 (0.104)
					1691 (0.112)
^{64}Cu	^{64}Ni(p,n)^{64}Cu	12.7 h	17.6 β^+	278.2	
			34 β^-		
^{61}Cu	^{61}Ni(*p,n*)^{61}Cu	3.33 h	61 β^+	523.7	656 (0.108)
	^{60}Ni(*d,n*)^{61}Cu				
^{60}Cu	^{60}Ni(*p,n*)^{60}Cu	23.7 m	93 β^+	872.0	826.4 (0.217)
				1324.9	1333 (0.880)
					1792 (0.454)
^{68}Ga	^{68}Zn(p,n)^{68}Ga	67.8 m	87.7 β^+	836	
^{66}Ga	^{66}Zn(p,n)^{66}Ga	9.49 h	56.0 β^+	1904	1039 (0.369)
					2752 (0.233)
^{45}Ti	^{45}Sc(p,n)^{45}Ti	3.08 h	84.2 β^+	439	
^{55}Co	^{56}Fe(p,2n)^{55}Co	17.53h	76 β^+	435.7 & 649.0	931.1 (0.75)
	^{54}Fe(d,n)^{55}Co				1409 (0.169)
	^{58}Ni(p,α)^{55}Co				
^{94m}Tc	^{94}Mo(*p,n*)^{94m}Tc	52.0 m	70.2 β^+	1094	871.1 (0.94)
^{44}Sc	^{44}Ca(p,n)^{44}Sc	3.97	94.3 β^+	632.0	1157 (0.999)
^{114m}In	^{114}Cd(p,n)^{114m}In→^{114}In	49.5 d	99.4 β^-	778.7	190.3 (0.156)
^{76}Br	^{76}Se(p, n)^{76}Br	16.2 h	55 β^+	1532	559.1 (0.74)
					657.0 (0159)
					1854 (0.147)

Several solid target systems for cyclotrons have been described earlier in the literature and examples of such systems can be found within the Journal of Applied Radiation and Isotopes (Lebeda et al., 2005; Thisgaard et al., 2011), Nuclear Instruments and Methods in Physics Research (Čomor et al., 2004; Steyn et al., 2013; Vereshchagin et al., 1993), Nuclear Medicine and Biology (McCarthy et al., 1997) and the International Workshop on Targetry and Target Chemistry proceedings (Avila-Rodriques et al., 2006; Gelbart et al., 2012).

Different solid target materials are typically in the form of foils, electroplated/sputtered plates or powder/metals pressed into an indentation within a backing. The target set up for production of different radionuclides is dependent on several things i.e. which reaction channels are available, the natural isotopic composition of the target material, the half-life of the desired product, threshold reactions for co-products etc. Several radionuclides can be accessed through different routes combining different particles with different target material (also energy threshold can be useful). As an example, production of ^{61}Cu ($T_{1/2}$=3.33 h, β^+=61%) (Rowshanfarzad et al., 2006) can be accessed via the ^{61}Ni(p,n)^{61}Cu reaction. The natural composition of Ni is ^{58}Ni(0.68), ^{60}Ni(0.26), ^{61}Ni(0.014),

^{62}Ni(0.036) and ^{64}Ni(0.0093). Therefore the ^{61}Ni(p,n)^{61}Cu reaction requires enrichment of the ^{61}Ni component to get any useful yields. This enriched material is expensive and will require recycling of the target material. Also foils made of the enriched ^{61}Ni are not commercially available so the expensive target material has to be purchased as a metal powder or similar. To increase the thermal heat conduction the powder is normally dissolved and then plated onto a backing of a good heat conductor like a gold disc (McCarthy et al., 1999). After irradiation the ^{61}Cu is separated by chemical means and the enriched material is recovered and re-plated on a disc ready for new irradiations. Another possible way to access ^{61}Cu is by irradiating, not so expensive, natural nickel with deuterons utilizing the ^{Nat}Ni(d,x)^{61}Cu reaction (Tolmachev et al., 1998) utilizing the relatively high isotopic ratio of ^{60}Ni (0.26) naturally occurring in Ni. The irradiation will lead to co-production of ^{62}Cu through the ^{60}Ni(d,n)^{62}Cu. The production is relatively small and even better is that the the co-produced ^{62}Cu has a short half-life (9.76 min) compared to ^{61}Cu (3.33 h) which makes it easy to wait for the decay of ^{62}Cu before using ^{61}Cu.

Another interesting radionuclide is ^{114m}In ($T_{1/2}$=45 d). This long lived radionuclide is listed as one of the emerging therapeutic radionuclides (IAEA, 2000). The ^{114m}In can be called a “cocktail radionuclide” since the decay of ^{114m}In involves emission of 190 keV-photons (suitable for SPECT and gamma camera monitoring) and high yields of conversion and Auger electrons. The main daughter radionuclide, ^{114}In (half-life 72 s), decays by emitting high-energy beta particles (mean energy 777 keV). The ^{114m}In can be produced from enriched ^{114}Cd utilizing the ^{114}Cd(p,n) ^{114m}In reaction. As an alternative natural foils (28.7 % ^{114}Cd) can be used if the simultaneously produced ^{110}In ($T_{1/2}$=69 min, β^+=62 %) and ^{111}In ($T_{1/2}$=2.8 d, Eγ= 171 keV, 90.2 % and 245 keV, 94 %) are allowed to decay. The produced ^{114m}In can be extracted by thermal diffusion technique, as was shown in Uppsala (Tolmachev et al., 2000), where the loss of the target material was less than 1%: opening up the possibility for re-use of the enriched target material. Later on the ^{114m}In-project was continued as a collaboration between Uppsala and Lund University (Bergqvist, 2006) with solid target designs matched to the Scanditronix cyclotron in Lund (fig 7.1).

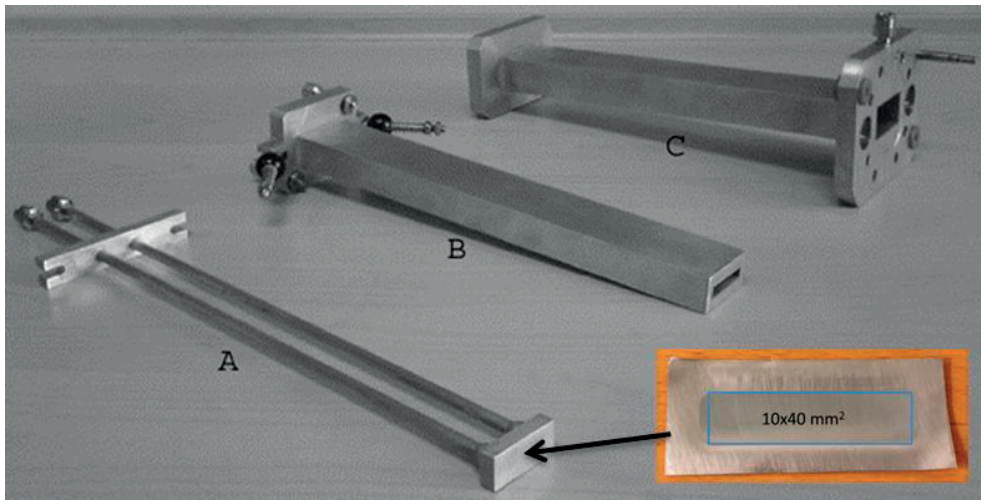

Fig 7.1:
The solid target for ^{114m}In-production constructed in Uppsala and matched to the MC 17 Scanditronix in Lund. The target holds cadmium foils.

The solid target design was further optimized and changed to utilize the thermal diffusion separation online, inside the target, during and after bombardment (Siikanen and Sandell, 2010). With this set up it was planned to use the beam-power, during irradiation, in combination with after-heating with thunderbolts to utilize the thermal diffusion separation of ^{114m}In from cadmium foils. However for most target types, the key performance parameter is the ability to effectively remove the heat deposited during the charged particle bombardment. Solid target materials that are good heat conductors can normally be aligned perpendicular to the charged particle beam. However at certain beam intensity-material combinations the beam power density will be problematic causing deterioration and burn holes in the target material. To compensate for these situations, and to improve the dissipation of heat that is generated from the beam, it is common to use an inclined plane to spread out the beam over a larger area and thereby reduce the power density in the beam strike area (fig 7.2).

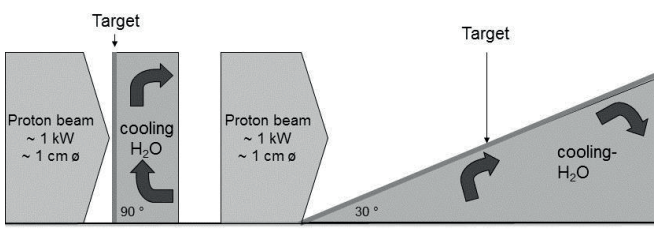

Fig 7.2:
To spread out the beam power, solid targets can be slanted.

7.2 Zirconium-89 (^{89}Zr)

The long biologic half-life of intact antibodies (1 to 3 weeks) requires use of radionuclides with similarly long half-lives, such as the positron-emitting radionuclide ^{89}Zr (Knowles and Wu, 2012). Zirconium-89 decays with a half-life of 78.4 h via both positron emission (22.7 %) and electron capture (73.3 %) to an intermediate ^{89m}Y state which in turn decays to stable ^{89}Y via a gamma ray emission (909 keV). The positron is emitted with mean positron energy of 396 keV (compare: 250 keV for ^{18}F). The sufficient high abundance of positrons makes this radionuclide well suited for antibody-tracking with PET.

The first production of ^{89}Zr was done in 1951 by Shure and Deutsch at M.I.T-cyclotron via Y(d,2n) reaction (Shure and Deutsch, 1951). The most common production route nowadays is via the ^{89}Y(p,n)^{89}Zr reaction. Attractive features, from a production point of view, with this reaction is that the target material is commercially available and naturally composed of monoisotopic ^{89}Y which results in relatively cheap targets and no requirement for material recovery. Figure 7.3 shows the cross sections for the reactions ^{89}Y(p,n)^{89}Zr, ^{89}Y(p,n)^{88}Zr and ^{89}Y(p,n)^{88}Y (Mustafa et al., 1988) as a function of proton energy. The co-production of long-lived ^{88}Zr ($T_{1/2}$=83 d) and ^{88}Y ($T_{1/2}$=107 d) can be avoided if the proton energy is lower than the energy-thresholds for ^{88}Zr and ^{88}Y production.

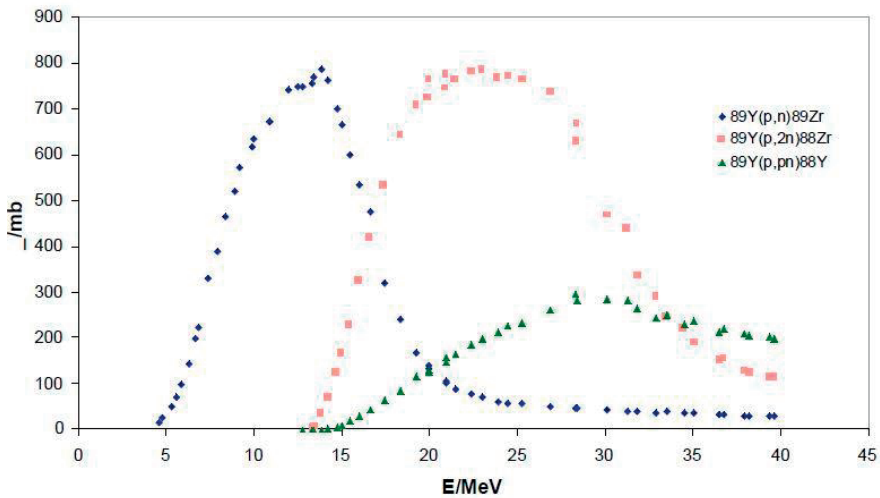

Fig 7.3:
Cross section dataset for the ^{89}Y(p,n)^{89}Zr reaction (energy range between 4.59 and 39.56 MeV) (Mustafa et al., 1988).

7.3 Solid target

7.3.1 Solid target design

The purpose of the work presented in paper III, was to develop a new solid target system for the MC 17 Scanditronix cyclotron. No solid targets were commercially available and no homebuilt solid targets had previously been developed for the cyclotron in Lund. In the design of the solid target it was attractive to have a system that:

- was flexible and could handle many different types of solid target material.
- had some adjustability in energy control to optimize MC 17 beam energy below or near threshold for competing reactions channels like (p,2n) reactions.
- was equipped with a remote handling of irradiated targets to minimize unnecessary exposure to personnel.

To separate the machine-vacuum from the target material and to hold a target inserting mechanism a docking station was constructed (fig 7.4). The docking station is a Scanditronix two-foil He-cooled flange which was modified to hold the target inserting mechanism. The two-foil He-cooled flange gives the possibilities to vary the beam energy by thickness-adjustment of the foils. The space between the two-foil He-Cooled flange and target inserting mechanism is constantly flushed with an inert gas during irradiation to maintain an inert environment. A schematic picture of the solid target system can be found in paper III.

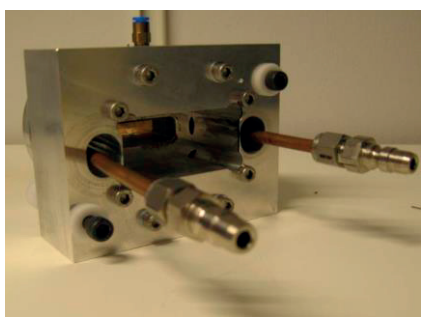

Fig 7.4:
The docking station is permanently mounted to the cyclotron, to hold the target inserting mechanism and to vary the beam energy by thickness-adjustment of the He-cooled foils.

The target inserting mechanism consists of a water cooled target holder piece (fig 7.5) which is mounted onto a pneumatic piston (fig 7.6). The inserting mechanism has a front plate with a beam entrance hole matched to the MC 17 beam profile (fig 7.7). The target inserting mechanism is connected to a special designed dedicated water system with one mode for cooling and one mode for vacuum which is used to grab and hold the target material. The latter makes it possible, when vacuum is switched off, to remotely drop activated foils, driven by gravity, into a lead pig. This remote handling of the activated targets minimizes the exposure to personnel. Targets are positioned onto the target holder piece and held with vacuum. They are then pressed against the front plate to seal the water cooling cavity against the target foil by compressing the O-ring. The target foils or backing that holds the target material should have a maximal area of 20x50 mm^2 to fit in the target inserting mechanism. The movable piston gives flexibility in the thicknesses (up to 80 mm) of foils, backing plates or holders for stacked targets. A detailed description of the system function can be found in paper III.

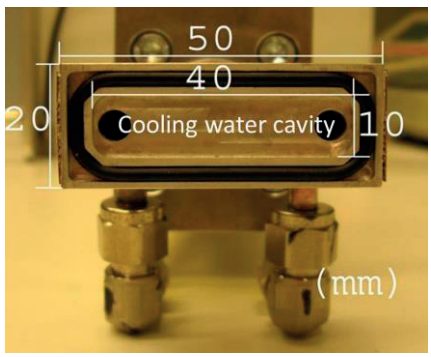

Fig 7.5:
Target holder piece with o-ring.

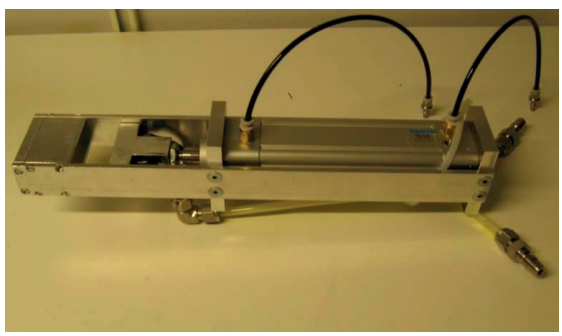

Fig 7.6:
The target inserting mechanism.

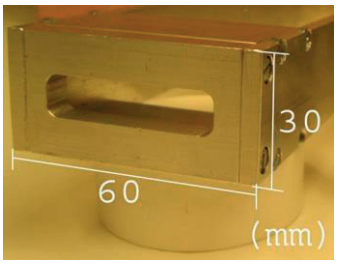

Fig 7.7:
Front plate with a 40x10 mm^2 beam entrance matched to the MC 17 beam profile.

Before the beam hits the actual target material it passes the front plate. Beam that passes outside the beam entrance window will hit the edges of the aluminum front plate. To avoid buildup of unwanted long lived radionuclides in the front plate, it was constructed from extra pure aluminum (alloy 6060) to reduce activation of alloy metals like copper ($^{65}Cu(p,n)^{65}Zn$, $T_{1/2}$=244.26 d), titanium ($^{48}Ti(p,2p)^{47}Sc$, $T_{1/2}$=3.35 d and $^{48}Ti(p,n)^{48}V$, $T_{1/2}$=15.97 d), iron ($^{56}Fe(p,n)^{56}Co$, $T_{1/2}$=77.27 d and $^{56}Fe(p,\alpha n)^{52}Mn$, $T_{1/2}$=5.59 d) etc.

7.3.2 Solid target performance

The target has performed very well with high reliability since it was installed in the beginning of 2008. The target performance has been demonstrated for production of ^{89}Zr thorugh the $^{89}Y(p,n)^{89}Zr$ reaction on monisotopic yttrium foils (50x20x0.64 mm^3). For optimization of ^{89}Zr-production the energy was decreased to 12.8 MeV with a 25 µm havar and a 200 µm silver foil combination inside the two-foil He-cooled window. With 12.8 MeV protons the co-production of longlived ^{88}Zr and ^{88}Y is minimized due to threshold for production and small cross sections (fig 7.3). The production yields were 2.2 ±0.2 GBq for 1 hour irradiation with 45 µA protons (n=13) or 6.3±0.06 GBq for 3 h irradiation with 45 µA (n=3).

To improve cooling we tested to place the foils in direct contact with the cooling water. Yttrium disolves in water and to investigate the impact from direct water cooling the target foils were placed into the target inserting mechanism with cooling water running for 72 h. The water had an effect on the foil with dissolved yttrium material all over the beam strike area, i.e. the surface in contact with water. However, only 2% mass weight of the yttrium foil could be scraped off after this test. The effect with beam on doesn't seem too harsh and the foils seems to tolerate many hours of beam and still only lose less than 1 % of the yttrium mass material as was determined when a foil was irradiated with 45 µA for 3 h (fig 7.8 and 7.9).

Fig 7.8:
A direct water cooled yttrium foil (50x20x0.64 mm^3) irradiated with 45 μA protons for 3 h.

Fig 7.9:
This picture shows the appearance of the yttrium foil from fig 7.8 after mechanical removal of green dissolved yttrium material. Less than 1 % mass weight was removed.

The only minor problems with the solid target so far have been a leakage in the two-foil He-cooled window which was repaired by replacing the two silver ring-sealing and the silver foil. Since then no other maintenance has been nessecary and the target has been operated without problems for more than 100 irradiations corresponding to more than 4500 μAh.

7.4 Separation module

7.4.1 Introduction

The production of one GBq of ^{89}Zr inside a 10x10x0.64 mm^2 yttrium foil will correspond to an extremely small amount, in the order of 10^{-7} magnitude, conversion of the original ^{89}Y atoms into ^{89}Zr atoms. To use the produced radionuclides they need to be separated from the bulk yttrium target material. Excellent reviews on ^{89}Zr-radiochemistry can be found in the literature, particularly those written by Vugts van Dongen at Vrije University in the Netherlands (Vugts and van Dongen, 2011), Severin and Nickles at the University of Wisconsin (Severin et al., 2011) and Deri and Lewis at the Memorial Sloan Kettering Cancer Center (Deri et al., 2013). Nowadays, the most common way to separate ^{89}Zr from yttrium is to use the weak cation exchange method using a hydroxamic acid resin. This was first performed by Meijs *et al. (Meijs et al., 1994)* utilizing their own-developed, custom-made hydroxamic acid resin from which the ^{89}Zr was eluted in oxalic acid. The purpose of the work presented in paper IV was to build an automated separation module for separation of ^{89}Zr produced in the solid target (paper III).

7.4.2 Separation module design and performance

The first separations carried out in Lund (Svensson, 2008) were based on a private visit to Amsterdam, following the paper by Verel et al (Verel et al., 2003). The initial simple set up, in Lund, consisted of lead bricks, manually operated three-port valves, syringes and tubing inside a ventilated fume hood (fig 7.10).

Fig 7.10:
Manual separation of ^{89}Zr from ^{89}Y foils in Lund.

After some manual hands-on-separations it was clear that the set-up could be optimized and automated with relay-controlled pinch-valves, tubing and a peristaltic pump to transfer the liquids back and forth (fig 7.11 and fig 7.12). The idea was realized by designing a module which consists of a simple peristaltic pump (Welco, 6-12 VDC) and 6 two way pinch valves (Takasago, 12 VDC) which are mounted on an aluminum plate (fig 7.13). On the upper side of the pinch valves, syringes and a packed column filled with home-made hydroxamate resin (Holland et al., 2009; Verel et al., 2003) were connected with Luer Lock tips to a Pharmed BPT tube (1 mm i.d and 3 mm o.d). On the lower side of the pinch valves the tubes were connected to a common line with 3 port valves. Before separation, 100 mg hydroxamate resin was manually activated and connected to the module. Also water and HCl-syringes were connected to the module before an irradiated yttrium foil was placed in the dissolving vial. The pinch valves and pump are controlled with an 8 channel USB relay card. To perform separations a valve/pump control sequence was programmed with Labview. The peristaltic pump is placed so that liquids on the right side of the pump can go to vials on the left side of the pump and vice versa by reversing the direction of the pump rotation. This setting was used to perform the separation similar to Holland et al. (Holland et al., 2009). Foils were dissolved by pumping from the syringe containing hydro chloric acid (fig 7.12) to the dissolving vial. After the foils were dissolved, the peristaltic pump direction was reversed and the solution was transfered to the hydroxamate resin where the ^{89}Zr was trapped and separated from yttrium and other metals. The elution of ^{89}Zr from the resin was done with oxalic acid.

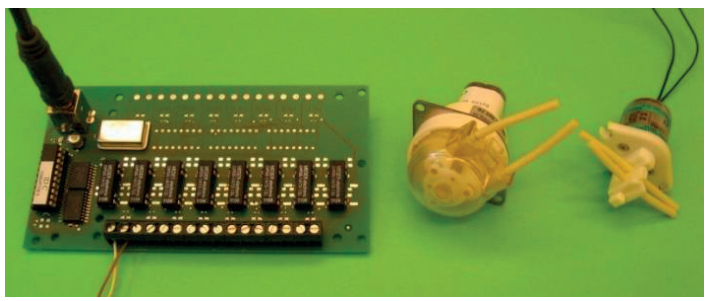

Fig 7.11:
Relay card, peristaltic pump and pinch valve used in the separation module.

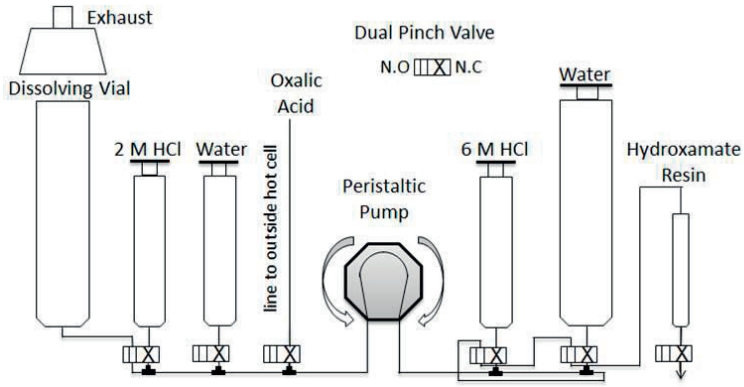

Fig 7.12:
A schematic picture describing the set-up of liquids, peristaltic pump and valves used for the module-aided separation of ^{89}Zr from yttrium foils. Reproduced with permission from [A peristaltic pump driven ^{89}Zr separation module AIP Conf. Proc. 1509, 206 (2012)]. Copyright [2015], AIP Publishing LLC.

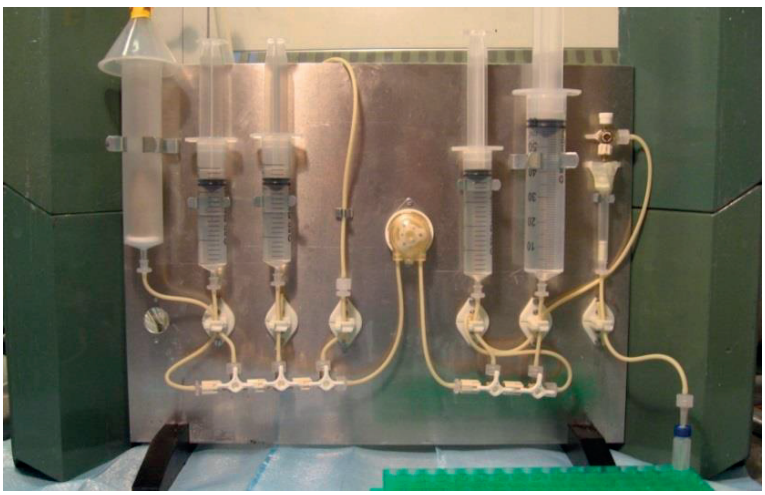

Fig 7.13:
The separation module in Lund. Reproduced with permission from [A peristaltic pump driven ^{89}Zr separation module AIP Conf. Proc. 1509, 206 (2012)]. Copyright [2015], AIP Publishing LLC.

In Lund the ^{89}Zr is normally produced in ~50x20x0.64 mm^3, ~3 g, yttrium foils with 45 μA, 12.8 MeV protons, utilizing the solid target system described in paper III. The entire procedure, from dissolution to collection of ten 200 μl ^{89}Zr fractions takes less than 90 min. More than 85% of activity measured in foil, (or 95% of transferred to resin) is collected in total of 2 ml oxalic acid. Approximately 10% of foil activity was trapped in the dissolving vial. The design of the module is simple and inexpensive. The automation reduces exposure to personnel, and reproduces

separation conditions precisely, which is helpful for sites with the aim to distribute large amounts of ^{89}Zr activity on a regular basis. All syringes, three port valves and tubes are disposables and can be changed before a new separation which is an attractive feature from a good manufacturing practice point of view. The flexibility of this type of module to take on separations of other radionuclides like ^{44}Sc has already been proven. (Valdovinos et al., 2015).

8 Preclinical experiments

8.1 Biodistribution and dosimetry of ^{89}Zr-labeled trastuzumab

8.1.1 Introduction

In 2010, 22 monoclonal antibodies (mAbs) (of which 19 are intact immunoglobulins) had been approved by the U.S Food and Drug Administration (FDA) for therapy, most of them for treatment of cancer (Reichert, 2008; Reichert and Valge-Archer, 2007). One of the FDA-approved antibodies is trastuzumab (Herceptin®). Trastuzumab is a monoclonal antibody specific for human epidermal growth factor receptor 2 (HER2) which is over expressed in certain types of aggressive breast cancer. Targeting human epidermal growth factor receptor 2 (HER2) using monoclonal antibodies has been a well-known therapeutic strategy for years. HER2 is involved in cell proliferation, cell division, angiogenesis, metastasis, and furthermore exerts antiapoptotic effects (Dijkers et al., 2010). The most commonly used methods for testing HER2 overexpression are using immunochemistry (IHC) or fluorescence *in situ* hybridization (FISH) at the time of diagnosis of the primary tumor (Wong et al., 2011). There is however data suggesting that HER2 expression may change over the course of treatment and that often different lesions in the same patient may not express HER2 to a similar degree (Rasbridge et al., 1994; Solomayer et al., 2006). Therefore it is encouraged in clinical guidelines to take biopsies throughout the course of treatment, which is an invasive and sometimes very difficult technique. Furthermore, it has been found that metastases from HER2 negative primary breast tumors can express HER2 and therefore respond to Trastuzumab treatment (Zidan et al., 2005). A biopsy sample of only the primary tumor could result in a false-negative diagnosis. To avoid sampling errors and to get a more complete picture, non-invasive techniques such as SPECT or PET imaging can instead be used to determine HER2 expression and localization of HER2-overexpressing lesions. This would relieve the patients of the stress of invasive procedures and provide clinical data about all lesions, giving healthcare professionals better opportunity for evaluating the progress over the course of treatment.

8.1.2 Radiolabeling and biodistribution of ^{89}Zr-trastuzumab in mice

The aims of this study (paper V) were to produce, separate and label ^{89}Zr to the monoclonal antibody trastuzumab. The labeled trastuzumab was injected in mice and the acquired biodistribution data was used for dosimetry calclulations. The ^{89}Zr used in the present trials was produced at the cyclotron unit in Lund, utilizing the solid target system described in paper III. For the first initial test-labeling and test-animals the ^{89}Zr was produced at Herlev University Hospital, Denmark, where zirconium was produced on an IBA Cyclone 18/9 H^- cyclotron using a COSTIS solid target system. Regardless if the ^{89}Zr was produced in Lund or Herlev, the separation was performed as earlier described using a hydroxamate resin and oxalic acid (Holland et al., 2009).

The radiolabeling of trastuzumab was performed according to the protocol by Vosjan et al.(Vosjan et al., 2010). Briefly, *p*-isothiocyanatobenzyl-desferroxamine (Df) (Macrocyclics, USA) was coupled to trastuzumab (Genentech). For radiolabeling, typically ~50-100 MBq of [^{89}Zr]Zr-oxalate was pH-adjusted to 7-7.1 with 2 M sodium carbonate and HEPES buffer and ~1 mg Df-trastuzumab was added to the ^{89}Zr-solution to get of ^{89}Zr-Df-trastuzumab. The reaction was incubated in room temperature for 1 h.

Biodistribution studies were conducted to evaluate the uptake of ^{89}Zr-Df-trastuzumab in HER2-expressing ovarian cancer cell line. Female immunodeficient nude mice Balb/C of 8-10 weeks age inoculated with SKOV3 cells (ATCC) tumors received 1 MBq ^{89}Zr-Df-trastuzumab through intravenous (i.v.) tail-vein injection. Animals were euthanized by intraperitoneal injection of Ketalar-Rompun solution At 2, 8, 24, 48, 72, 168 and 240 h (5 animals/time point) pi. Blood and organs including tumor were taken, weighed and their radioactivity were measured in a NaI(Tl) well counter (1480 Wizard, Wallac). The organ specific uptake values were calculated as percentage injected activity per gram tissue (%IA/g).

8.1.3 Dosimetry

The measured uptake values for the individual organs were plotted and fitted with a bi-exponential activity function. From the fitted curves the cumulated activity, $\tilde{A}_{rs}$, was calculated by integration:

$$\tilde{A}_{r_S} = \int_0^\infty A_{r_s}(t)dt$$

Absorbed mean doses were calculated according to the MIRD-scheme (Bolch et al., 2009), stating that the mean absorbed dose from a source region r_S to a target region r_T can be described as:

$$\overline{D}(r_T \leftarrow r_S) = \tilde{A}_{r_S} \cdot S(r_T \leftarrow r_S)$$

The S-value depends on radiation type, energy emitted and the geometry. The S-values were calculated by Monte Carlo using MNCP and a realistic mouse phantom (MOBY), which has been described elsewhere (Larsson et al., 2011; Larsson et al., 2007). For human dosimetry the OLINDA computer code (Stabin et al., 2005) was used to estimate absorbed and effective doses in humans using the MIRD phantom in combination with the acquired kinetics from the collected mice biodistribution data.

8.1.4 Results

Uptake of radioactivity decreased over time in all organs after injection, except the salivary glands and tumor tissue. The high absorbed dose to the bone marrow can be explained by the fact that zirconium is a bone seeker (Abou et al., 2011) and will, when not tightly bound to another molecule accumulate in the bones. The accumulation of ^{89}Zr in bones indicates that the Df-chelation is not perfect. The calculated effective dose was 0.3 mSv/MBq when transferring the murine residence times to humans. An example of PET/CT image of SKOV3 xenografts measured 3 days post-injection of ^{89}Zr-Df-trastuzumab is shown in figure 8.1. The tumor in the hind leg was well visualized.

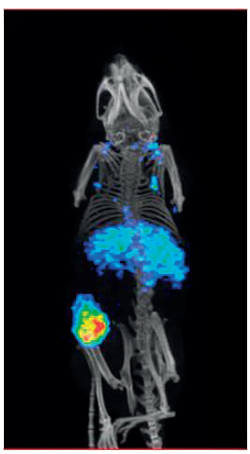

Fig 8.1:
Micro-PET image of a mouse 3 days post injection clearly showing tumor uptake, along with smaller amounts of uptake in liver.

8.2 Estimation of MR_{glc} in mice with ^{18}F-FDG

8.2.1 Introduction

The introduction of new chemotherapy-drugs or radionuclide therapies requires large clinical studies. Even if a therapy is proven to be efficient in a larger group, the individual therapy response can vary considerably and it is of clinical value to be able to predict tumor response and distinguish responders from non-responders before or, at least early, during treatment. One method, promising for such predictions, is to use 2-[^{18}F]fluoro-2-deoxy-D-glucose-positron emission tomography (^{18}F-FDG-PET).

The ^{18}F-FDG molecule carries one radioactive [^{18}F] in position 2. The ^{18}F-FDG uses the same pathway into the cell as glucose. Inside the cell, ^{18}F-FDG is metabolized, only one step, to 2-^{18}FDG-6-PO_4 that remains trapped inside the cell. The concentration of radioactive metabolites grow with time in proportion to the cells metabolism of glucose. This results in a greater accumulation of ^{18}F-activity in tissues where the glucose metabolism is higher than for normal tissues (e.g. many cancers). The activity distribution can then be detected and visualized by a PET-camera.

The ^{18}F-FDG-PET is an established method for evaluation of metabolic response following cytotoxic therapy. Early metabolic response during chemotherapy in Hodgkins lymphoma, detected by ^{18}F-FDG-PET examination, is proven to correlate to therapy outcome in Hodgkins lymphoma (Avigdor et al., 2010; Zinzani et al., 2006) and also in other tumors although not as convincing (Janssen et al., 2012). The predictive value of early metabolic response in other tumors has yet to be clinically established in order to introduce sequential PET studies for monitoring cytotoxic treatment (Weber, 2009). To accomplish this, it is important to gain basic knowledge of metabolic tumor effects of cytotoxic drugs in experimental studies for example by using human xenografts in mice.

Earlier studies on mice have reported the importance of careful handling of the mice to reach optimal conditions for ^{18}F-FDG measurements. It has been shown that fasting before the PET scan and warming of mice before and after injection of ^{18}F-FDG is crucial (Fueger et al., 2006). Parameters such as, temperature, dietary state and type of anesthesia have been investigated and are found to interfere with blood glucose levels and ^{18}F-FDG kinetics (Flores et al., 2008; Kilbourn et al., 1985; Lee et al., 2005; Woo et al., 2008). If the animal handling during the experiments induces elevated blood glucose levels, this may result in a non-normal physiological state which interferes with the ^{18}F-FDG uptake in tumor cells, in humans as well as in mice (Lindholm et al., 1993; Wahl et al., 1992). Complete

surgical anesthesia prior to PET scans is not needed, but a sufficient depth of anesthesia to avoid disturbing muscle activity is important. One of the most common anesthesia in experimental animal models is Ketamine-xylazine but this anesthesia is known to induce hyperglycemia (Saha et al., 2005). In 1984, Flecknell and Mitchell (Flecknell and Mitchell, 1984) concluded that fentanyl-fluanisone in combination with midazolam or diazepam, given intraperitoneally, was preferable if surgical anesthesia and muscle relaxation is desired in different laboratory animals.

8.2.2 Standardized Uptake Value (SUV)

There are different ways to assess tissue activity with ^{18}F-FDG-PET and the most common are based on different types of standardized uptake values (SUV). SUV is a semi-quantitative analysis in which the tumor ^{18}F-FDG concentration is normalized to the amount of the injected activity and body weight.

$$SUV_{BW} = \frac{C_{PET}(T)}{A/weight}$$

Where $C_{PET}(T)$= is the tissue activity concentration (for example in MBq/mL) and administered activty, A (in MBq) divided by body weight (usually in kg)
Instead of the body weight the injected activity can be corrected by the lean body mass (LBM) (Tahari et al., 2014) or the body surface area (BSA) (Kim et al., 1994).

$$SUV_{BSA} = \frac{C_{PET}(T)}{A/BSA}$$

The different formulas for calculating BSA are found in Verbraecken et al. (Verbraecken et al., 2006).

The SUV is easy to perform but it is sensitive to several sources of variability like body composition and habitus, length of uptake period, plasma and glucose levels. (Hamberg et al., 1994; Huang, 2000; Keyes, 1995) and therefore the use of SUV for quantitative purposes should be treated carefully. The reason for the continuous usage of SUV is that dynamic imaging and cumbersome blood sampling are not necessary.

8.2.3 Metabolic Rate of glucose (MR_{glc})

The metabolic rate of glucose (MR_{glc}) is a parameter providing quantitative information about tumor metabolism and, in contrast to SUV, calculation of MR_{glc},

either with nonlinear regression (Phelps et al., 1979) or Patlak analysis (Patlak et al., 1983) are based on measurements of the rate of glucose uptake over time. Both methods are based on the three-compartment model for measurement of metabolic rate for glucose with ^{14}C-DG (^{14}C-2-Deoxy-D-glucose) originally developed by Sokoloff et.al (Sokoloff et al., 1977). The extended model for measurement of cerebral metabolic rate for glucose with ^{18}F-FDG as developed by Phelps et al (Phelps et al., 1979) includes the k_4^*mediated hydrolysis of ^{18}F-FDG-6-PO_4 back to ^{18}F-FDG+PO_4 (fig 8.2).

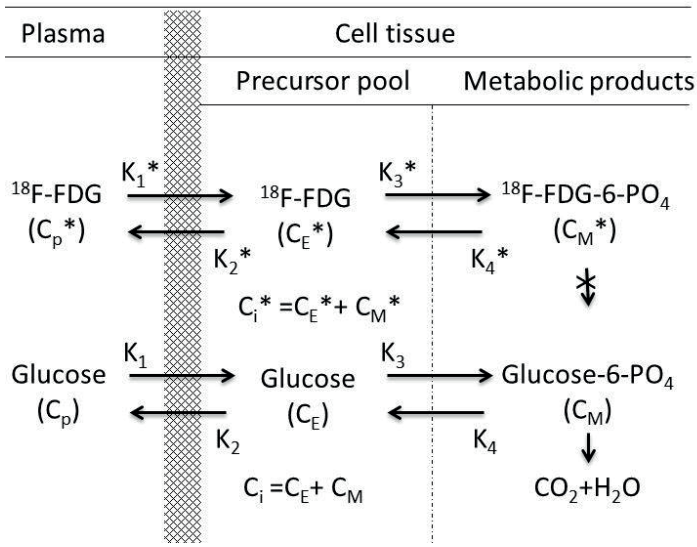

Fig 8.2:
The three compartment model for measurement of metabolic rate for glucose with ^{18}F-FDG as developed by Phelps et al in which they included the k_4* mediated hydrolysis of ^{18}F-FDG-6-PO_4→^{18}F-FDG+PO_4 . The model originally developed by Sokoloff et all only considered k_1*, k_2* and k_3*. The C_i* represents total ^{18}F concentration in tissue, the C_E*and C_M*represents ^{18}F-FDG and ^{18}F-FDG-6-PO_4 concentrations in tissue whereas C_p* is the plasma concentration of ^{18}F-FDG. Representation without asterix is related to glucose.

Later on Patlak et al developed a graphical analysis to determine MR_{glc}. By plotting Ci*(t)/C_p*(t) versus $\int C_p^*(t')dt'$)/C_p*, a part of the graph will yield a straight line. The slope from this curve, K_i, then represent K_i=K_1*K_2*/(K_2*+K_3*) and the metabolic rate can be calculated from MR_{glc}=K_iC_{gl}/LC. Where the lumped constant (LC) represents the difference in transport and phosphorylation between glucose and ^{18}F-FDG and C_{gl} is the blood glucose level.

In small animal imaging, measurements of the rate of glucose uptake over time are demanding because of the rapid and frequent blood sampling. Nevertheless, the importance of getting the most accurate measurement of the tumor metabolism overrides the effort. However in paper VI we aimed to utilize an intraperitoneal

injection (i.p) of ^{18}F-FDG which results in a slower rise of the input function compared to intravenous injection (i.v). This was used in combination with a modified autoradiographic formula, previously described by Rhodes (Rhodes et al., 1983) for the estimation of MR_{glc}.

$$MR_{glc} = \frac{C_{gl} \cdot Ci\,(T)}{LC \cdot \int_0^T Cp\,(t)dt} \qquad \text{eq.8.1}$$

The formula is based on a 3-compartment model where LC is the lumped constant, C_{gl} is the blood glucose value, C_i is activity in tissue, T is the time point post injection and $C_p(t)$ is the plasma ^{18}F-FDG concentration as a function of time.

Equation 8.1 only requires one PET-scan at approximately 60 minutes after the injection of ^{18}F-FDG. It assumes that all radioactivity in the tissue is composed solely of 2-^{18}FDG-6-PO_4, no non-phosphorylated ^{18}F-FDG and that the dephosphorylation of 2-^{18}FDG-6-PO_4 is negligible. A similar equation, which corrects for the free non-phosphorylated ^{18}F-FDG has also been published by Brooks (Brooks, 1982). A prerequisite for using both these calculations is stable blood glucose levels during the acquisition time and therefore we aimed to find an i.p anesthesia which kept the animals sedated with a stable and also a low blood glucose level.

The aims of paper VI were to:

1) Establish an easy and robust i.p anesthesia resulting in low and stable blood glucose levels useful for ^{18}F-FDG-PET single scans, i.e. autoradiographic measurements, for the estimation of metabolic rate of glucose (MR_{glc}) in mice.

2) To optimize the experimental setting for sequential ^{18}F-FDG studies by looking at blood sampling frequency and the well-being of animals exposed to the chosen anesthesia.

3) To validate the method by determining cerebral MR_{glc} values in mice exposed to the experimental setting and compare them to the literature.

Several anesthesia agents were tested and evaluated for b-glucose level (absolute level and stability), well-being of the animals, sedation capacity (time) before choosing the fentanyl-fluanisone and diazepam-combination. Both the anesthesia and the ^{18}F-FDG were administered intraperiotenally (I.P). For the ^{18}F-FDG this resulted in a slower rise of the input function, making the blood sampling less stressful and less sensitive to the exact timing of the sampling. Contrastingly, for i.v-injections it is important to have a more frequent sampling interval in the

beginning of the time activity curve to “catch” the rapid rise of the blood activity peak.

When stable experimental conditions were obtained, we carried out a sequential experiment where the well being of tumor bearing mice were studied at three time points, one before chemotherapy and on days 2 and 8 after chemotherapy. The experimental setting was well tolerated. All mice could carry out three rounds of anesthesia (with full blood sampling) as well as the cytotoxic therapy.

To validate the method, average whole brain and cerebellum MR_{glc} were determined and translated to occipital (72.7 μmol $100g^{-1}$ min^{-1}) and parietal cortex (76.1 μmol $100g^{-1}$ min^{-1}) by using ratios from average whole brain to occipital and parietal cortex in rats (Phelps et al., 1986). Mouse MR_{glc} in occipital and parietal cortex brain has previously been reported as approximately 70 μmol $100g^{-1}$ min^{-1} (conscious mice) using the 2-^{14}C-DG autoradiographic method (Sokoloff 1977). When ketamine/xylazine anesthetics were applied the MR_{glc} decreased to approximately 40 μmol $100g^{-1}$ min^{-1} (Toyama et al., 2004). In this study LC=0.62, which is valid for brain, was used. For most tumors the LC-value is still unknown and therefore the absolute number of the MR_{glc} in the tumors cannot be determined. However, if the LC-value for a specific tumor type is assumed to be the same in different individuals it should be possibilble to conduct both intra- and interindividual measurements without knowing the actual correct LC-value. This would be useful in longitudinal tumor studies focusing on therapeutic effects of cytotoxic treatment.

9 Conclusions and future work

In Lund the development of the water target (paper I) increased the production capacity by a factor of 3 (from step 3 to step 4 in fig 9.1) which was a very important improvement at this critical time with the installations of two new combined PET/CT cameras in Lund and Malmö. Besides providing ^{18}F-FDG to Lund, Malmö, Göteborg and Växjö on a daily basis the "Lund-target" has also had a national-international impact. With the installations on MC 17 cyclotrons in Uppsala (modified to circular beam), Groningen, Toronto, Taipei, St Petersburg and Copenhagen (MC 32, modified to circular beam) this improved water target was clearly a necessary and helpful development for sites using Scanditronix machines.

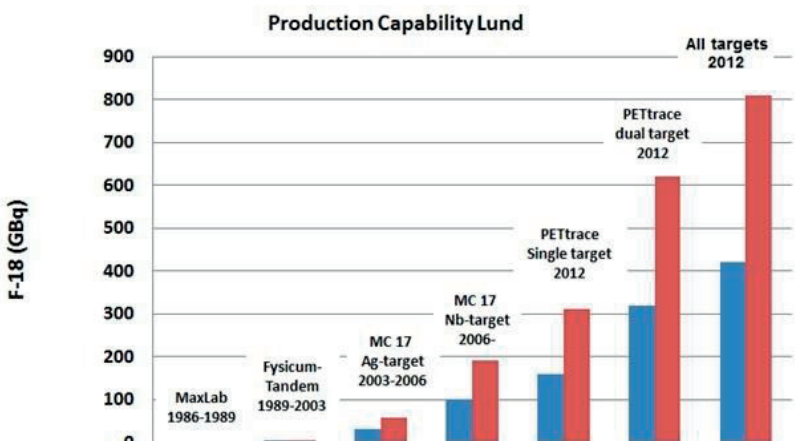

	1	2	3	4	5	6	7
1 h irradiation	0,01	3,5	30	100	160	320	420
2 h irradiation	0,025	5,7	56	190	310	620	810

Fig 9.1:
The figure describes the increase of [^{18}F]Fluoride production capacity in Lund from photon activation of sodium to the usage of two (GE PETtrace & MC 17) cyclotrons simultaneously

Today most people involved in routine production of ^{18}F-FDG are satisfied with the performance of niobium water targets. They are robust, reliable, does not require excessive maintenance and niobium is not activated too much. The last problem to solve with the water targets is to find a better foil material in order to reduce the exposure orginating from activation in havar.

In paper II it was highlighted that routine production targets can also be used as a rather intense source of fast neutrons (10^{10}-10^{11} n $cm^{-2}s^{-}1$) useful for small scale activation of target foils simply by placing them on the backside of the production target. This gives a cyclotron facility convenient access to an occasional neutron source that can easily be switched on and off.

In the beginning of the development of PET the majority of clinical and basic science research was focused on radiopharmaceuticals based on the ubiquitous isotopes ^{11}C, ^{13}N-, ^{15}O-, and ^{18}F. However recent research especially in antibody-based cancer therapeutics has opened up a concomitant research in finding companion diagnostics for these therapies (Deri et al., 2013). To access more un-conventional radionuclides a solid target system was developed (paper III) and tested for production of ^{89}Zr. Table 9.1 shows comparisons with other academic sites and their outputs of ^{89}Zr. The values were calculated from data found in the given references. It should be highlighted that for ^{89}Zr production it is preferable to use proton energy below 13.1 MeV to avoid co-production of ^{88}Zr which cannot be chemically separated from ^{89}Zr.

Table 9.1: To compare the experimental production results with theoretical result the latter is calculated with a MATLAB-script. This script utilizes already published cross sections for the $^{89}Y(p,n)^{89}Zr$ reaction (Mustafa et al., 1988) and stopping power values generated from SRIM-code (Ziegler et al., 2010).

Production Site	Ep (MeV)	Theoretical (MBq/μAh)	Measured (GBq/μAh)	Yield	Reference
Herlev	14.8	79	69	87 %	Paper V
Lund	12.8	57	50	88 %	Paper III
New York	15	88	55	63 %	(Holland et al., 2009)
Amsterdam	14	74	53	72 %	(Meijs et al., 1994)

The "^{89}Zr-factory"was further streamlined by the development of an automated separation module (paper IV). The flexibility of this type of module to take on separations of other radionuclides like ^{44}Sc has already been proven. (Valdovinos et al., 2015).

In the first preclinical experiment (paper V) the produced and separated ^{89}Zr was tested for radiolabeling of an antibody that targets HER2 receptors. Expression of

these receptors are associated with aggressive breast cancer and this type of breast cancer can be treated with immuno-therapy using trastuzumab antibodies. However for the treatment to have an effect the receptors need to be present. By labeling a small amount of the same antibody with ^{89}Zr, a non-invasive immunoPET can verify the presence of HER2 before an expensive full treatment is started. In paper V this was done on a preclinical level but the goal is to translate the same concept into the clinic.

In the second preclinical experiment (paper VI) an anesthetic protocol for determination of MR_{glc} in mice with ^{18}F-FDG was developed. The introduction of new chemotherapy-drugs or radionuclide therapies requires large clinical studies. Even if a therapy is proven to be efficient in a larger group, the individual therapy response can vary considerably and it is of clinical value to be able to predict tumor response and distinguish responders from non-responders before or, at least early, during treatment. One method, promising for such predictions, is to use ^{18}F-FDG-PET. Before introducing new chemotherapy drugs into the clinic it is important to gain basic knowledge of metabolic tumor effect and such information can be acquired with experimental studies for example by using human xenografts in mice.

The work presented in this thesis has increased the use and broadened the access of radionuclides by the development of a water and solid target system. The radionuclides produced in the targets are already used routinely in the clinic or are currently in a pre-clinical step before they can be introduced for human use. The work presented in the thesis will hopefully inspire other sites to devlop their own target systems or translate the systems presented here to match their own machines.

10 Acknowledgement

Thank you to everyone who has helped me along the way. The never ending support from my supervisor, co-supervisor, colleagues, parents, family, and friends has had a strong and positive influence in my accomplishment of this thesis. Thank you

I wish to express my deepest gratitude to my main supervisor Anders Sandell who is one of the most interesting persons I have ever met. To have been tutored by you and to have worked with you has been really fun and I am very grateful that you believed in me and that you shared your knowledge. I will always appreciate our discussions about everything, problem solving with MC 17 and all our fun conferences, meetings and trips over the bridge.

Sven-Erik Strand, my co-supervisor, for all your support, for being an amazing professor and for introducing me to the exciting world of nuclear medicine. Without your optimism, guidance, contact-net and help this thesis would not have been written.

Tomas Olsson, head of the Nuclear Medicine unit at Lund hospital, for all the support and for inspiring me to go to conferences to present our research during all the years I worked part time at the Cyclotron Unit in Lund.

Mikael Peterson for all the help, the backup during early mornings running the cyclotrons, fruitful discussions from since we were 5 years until now sharing an office in Lund. I hope I see you next to me in another office soon.

Thuy Tran for all the fun, our collaborations and for introducing me to the cell and radiolabeling field. Without you I could never know that our ^{89}Zr was actually useful.

all my teachers, friends and colleagues at MSF for the education and for all the nice days in school. Particular acknowledgment goes to the SST group and PhD-student gang; Michael Ljungberg, Bo-Anders Jönsson, Katarina Sjögreen-Gleisner, Erik Larsson, Ronnie Wirestam, Lena Jönsson, Bertil Persson, Linda Knutsson, Anders Örbom, Anders Nilsson, Gustav Brolin, Gustav Grafström, Filip Szczepankiewicz, Johan Gustafsson, Jonas Ahlstedt, Anders Nilsson, Anna Stenvall, Katarina Sjögreen-Gleisner, Kaj Ljunggren, Suaad Meerkhan, Emma Mellhammar, Oskar Vilhelmsson Timmermand, Pontus Kjellman, Renata Madru,

Andre Ahlgren, Anna Rydhög, Anneli Edvardsson, Emelie Lindgren, Hunor Benedek, and Mårten Dalaryd.

my colleagues at the Cyclotron Unit; Birgitta, Susanne, Berit, Kristin, Monica, Petter, Balint, Karin, Martina, Eleonora, Staffan, Stefan, Joachim and Nadja for the team work during the early FDG-mornings and for all the fun times for so many years.

Professor Mikael Jensen, Risö DTU for all the valuable input regarding many of my manuscripts, for letting me go to CERN and for being a very inspiring person in my field.

Jesper Fonslet, Risö DTU, for all the fun, for all our struggling in our collaborations.

Dr Gregory Severin, Risö DTU for all the collaborations and for reading and correcting this summary.

In particular, acknowledgements are extended to all of the co-authors of the papers for providing expertise in different fields.

Johanna Sjövall, Eva Brun and Elisabeth Kjéllen for all the help over the years, for our collaborations and for being my link to the medical doctor world.

The work presented in this thesis would not have been possible without help from: Jan Hultqvist for machining separation module and target parts, Joachim Schultz for help with targets, Lars Ekblad, Margaretha Olsson, Camilla Ekenstierna and Catarina Blennow for assistance with the animal studies, Per Roos, Risö DTU, for ICPM measurements, Ulrika Svanholm for correcting paper III, Erik Larson and Gustav Brolin for many discussions and help with different stuff.

Dr Jonathan Engle, Los Alamos, for helping me to go and live in Madison where I had the great opportunity to work with Professor R.J Nickles and to hang out with one of the best cyclotron gangs in the world. Thank you very much Jerry, Todd, Hector, Reinier, Paul, Stephen, Weibo, Hao, Yin and Mo. My stay with you is a very nice memory for the rest of my life!

Dr. Holger Jensen, Copenhagen, and Joachim Schultz, Uppsala, for continuous friendship and for all the fun meetings in Copenhagen and other places.

my friends Erik and Cherry in Lund for housing, feeding and taking extra care of me when I needed it the most to finish some experiments after moving away from Lund.

sjukhusfysikermaffian Daniel, Johan, Emil, Christoffer and lillDanne for the student years and for many years to come.

my new physicist colleagues; Cathrine Jonsson, Lars Ideström, Alejandro Sánchez Crespo, Disa Åstrand, Oscar Ardenfors, Joachim Nilsson and the rest of the gang

at Karolinska hospital, Stockholm for all the support in finishing my thesis and for a very interesting future to come.

I want to thanks my parents Jarmo and Barbro for bringing me to the world and for giving me love and interest for nature science. Great job! I want to thank my sister Jessica with Alexander and my niece Olivia. I want to thank my brother Jonas with Fresia for many fun years in Lund now continuing in Stockholm. I want to thank my niece Luna for shining like a moon every day

I want to thank my love and Spanish ray of light, Anna and her wonderful family. Thank you guapa it is amazing to have you in my life!

The work presented in this thesis was generously supported by; Swedish Cancer Society, Mrs. Berta Kamprad Foundation, Gunnar Nilsson Cancer Foundation, John and Augusta Person Foundation, Medical faculty ALF grants, Inga Britt and Arne Lundberg Foundation, and the Swedish Research Council, Foundations of Lund University Hospital, the King Gustaf V Jubilee Fund, government funding of clinical research within the Swedish National Health Service, Region of Scania R&D Funding, Thank you!

11 References

Abou, D.S., Ku, T., Smith-Jones, P.M., 2011. In vivo biodistribution and accumulation of 89Zr in mice. Nuclear medicine and biology 38, 675-681.
Avigdor, A., Bulvik, S., Levi, I., Dann, E.J., Shemtov, N., Perez-Avraham, G., Shimoni, A., Nagler, A., Ben-Bassat, I., Polliack, A., 2010. Two cycles of escalated BEACOPP followed by four cycles of ABVD utilizing early-interim PET/CT scan is an effective regimen for advanced high-risk Hodgkin's lymphoma. Annals of Oncology 21, 126-132.
Avila-Rodriques, M.A., Nye, J.A., Nickles, R.J., 2006. Production of Metallic Radionuclides on an 11 MeV Cyclotron, Eleventh International Workshop on Targetry and Target Chemistry.
Bergqvist, E., 2006. Construction of Target Holder for Production of 114mIn from thin 114Cd foils with MC16 Proton Cyclotron Master of Science Program in Engineering Physics Uppsala University, Uppsala.
Berridge, M.S., Kjellstrom, R., 1989. Fluorine-18 production: New designs for 0–18 water targets. Journal of Labelled Compounds and Radiopharmaceuticals 26, 188-189.
Berridge, M.S., Voelker, K.W., Bennington, B., 2002. High-yield, low-pressure [18O] water targets of titanium and niobium for F-18 production on MC-17 cyclotrons. Applied radiation and isotopes : including data, instrumentation and methods for use in agriculture, industry and medicine 57, 303-308.
Blessing, G., Coenen, H.H., Franken, K., Qaim, S.M., 1986. Production of [18F]F2, H18F and 18Faq− using the 20Ne(d, α)18F process. International Journal of Radiation Applications and Instrumentation. Part A. Applied Radiation and Isotopes 37, 1135-1139.
Bolch, W.E., Eckerman, K.F., Sgouros, G., Thomas, S.R., 2009. MIRD pamphlet No. 21: a generalized schema for radiopharmaceutical dosimetry--standardization of nomenclature. Journal of nuclear medicine : official publication, Society of Nuclear Medicine 50, 477-484.
Bosko, A., 2005. General electric PETtrace cyclotron as a neutron source for boron neutron capture therapy, Texas A&M University.
Bosko, A., Zhilchenkov, D., Reece, W.D., 2004. GE PETtrace cyclotron as a neutron source for boron neutron capture therapy. Applied radiation and isotopes : including data, instrumentation and methods for use in agriculture, industry and medicine 61, 1057-1062.

Brooks, R.A., 1982. Alternative formula for glucose utilization using labeled deoxyglucose. Journal of nuclear medicine : official publication, Society of Nuclear Medicine 23, 538-539.
Casella, V., Ido, T., Wolf, A.P., Fowler, J.S., MacGegor, R.R., Ruth, T.J., 1980. Anhydrous F-18 Labeled Elemental Fluorine for Radiopharmaceutical Preparation. Journal of Nuclear Medicine 21, 750-757.
Clark, J.C., Silvester, D.J., 1966. A cyclotron method for the production of fluorine-18. The International journal of applied radiation and isotopes 17, 151-154.
Čomor, J.J., Stevanović, Ž., Rajčević, M., Košutić, D., 2004. Modeling of thermal properties of a TeO2 target for radioiodine production. Nuclear Instruments and Methods in Physics Research Section A: Accelerators, Spectrometers, Detectors and Associated Equipment 521, 161-170.
Crouzel, C., Comar, D., 1978. Production of carrier-free 18F-hydrofluoric acid. The International journal of applied radiation and isotopes 29, 407-408.
Deri, M.A., Zeglis, B.M., Francesconi, L.C., Lewis, J.S., 2013. PET imaging with 89Zr: from radiochemistry to the clinic. Nuclear medicine and biology 40, 3-14.
Dijkers, E.C., Oude Munnink, T.H., Kosterink, J.G., Brouwers, A.H., Jager, P.L., de Jong, J.R., van Dongen, G.A., Schroder, C.P., Lub-de Hooge, M.N., de Vries, E.G., 2010. Biodistribution of 89Zr-trastuzumab and PET imaging of HER2-positive lesions in patients with metastatic breast cancer. Clinical pharmacology and therapeutics 87, 586-592.
Ehrlich, P., On immunity, with special reference to cell-life (Croonian Lecture, Royal Society of London, 1990), reprinted in Collected Papers of Ehrlich P, vol 2, ed Himmelweit, New York
Engle, J.W., Lopez-Rodriguez, V., Gaspar-Carcamo, R.E., Valdovinos, H.F., Valle-Gonzalez, M., Trejo-Ballado, F., Severin, G.W., Barnhart, T.E., Nickles, R.J., Avila-Rodriguez, M.A., 2012. Very high specific activity 66/68Ga from zinc targets for PET. Applied radiation and isotopes : including data, instrumentation and methods for use in agriculture, industry and medicine 70, 1792-1796.
Fitschen, J., Beckmann, R., Holm, U., Neuert, H., 1977. Yield and production of 18F by 3He irradiation of water. The International journal of applied radiation and isotopes 28, 781-784.
Flecknell, P.A., Mitchell, M., 1984. Midazolam and fentanyl-fluanisone: assessment of anaesthetic effects in laboratory rodents and rabbits. Laboratory animals 18, 143-146.
Flores, J.E., McFarland, L.M., Vanderbilt, A., Ogasawara, A.K., Williams, S.P., 2008. The effects of anesthetic agent and carrier gas on blood glucose and tissue uptake in mice undergoing dynamic FDG-PET imaging: sevoflurane and isoflurane compared in air and in oxygen. Molecular imaging and biology : MIB : the official publication of the Academy of Molecular Imaging 10, 192-200.
Fowler, J.S., MacGregor, R.R., Wolf, A.P., Farrell, A.A., Karlstrom, K.I., Ruth, T.J., 1981. A shielded synthesis system for production of 2-deoxy-2-[18F]fluoro-

D-glucose. Journal of nuclear medicine : official publication, Society of Nuclear Medicine 22, 376-380.
Fritzler, S., Maika, V., Grillon, G., Rousseau, J.P., Burgy, F., Lefebvre, E., d'humières, E., McKenna, P., Ledinqham, K.W.D., 2003. Proton beams generated with high-intensity lasers: Applications to medical isotope production. Applied Physics Letters 83, 3039.
Fueger, B.J., Czernin, J., Hildebrandt, I., Tran, C., Halpern, B.S., Stout, D., Phelps, M.E., Weber, W.A., 2006. Impact of animal handling on the results of 18F-FDG PET studies in mice. Journal of nuclear medicine : official publication, Society of Nuclear Medicine 47, 999-1006.
Gelbart, W., Johnson, R.R., Abeysekera, B., 2012. Solid target irradiation and transfer system. AIP Conference Proceedings 1509, 141-145.
Guillaume, M., Luxen, A., Nebeling, B., Argentini, M., Clark, J.C., Pike, V.W., 1991. Recommendations for fluorine-18 production. International Journal of Radiation Applications and Instrumentation. Part A. Applied Radiation and Isotopes 42, 749-762.
Hagedoorn, H.L., Verster, N.F., 1963. The magnetic field of a two-particle fixed-energy AVF cyclotron without trimming coils, Proceedings of the International Conference on Sector-Focused Cyclotrons and Meson Factories, Geneva, pp. 286-290.
Hamacher, K., Coenen, H.H., Stocklin, G., 1986. Efficient stereospecific synthesis of no-carrier-added 2-[18F]-fluoro-2-deoxy-D-glucose using aminopolyether supported nucleophilic substitution. Journal of nuclear medicine : official publication, Society of Nuclear Medicine 27, 235-238.
Hamberg, L.M., Hunter, G.J., Alpert, N.M., Choi, N.C., Babich, J.W., Fischman, A.J., 1994. The dose uptake ratio as an index of glucose metabolism: useful parameter or oversimplification? Journal of nuclear medicine : official publication, Society of Nuclear Medicine 35, 1308-1312.
Holland, J.P., Sheh, Y., Lewis, J.S., 2009. Standardized methods for the production of high specific-activity zirconium-89. Nuclear medicine and biology 36, 729-739.
Holland, J.P., Williamson, M.J., Lewis, J.S., 2010. Unconventional Nuclides for Radiopharmaceuticals. Molecular Imaging 9, 1-20.
Huang, S.C., 2000. Anatomy of SUV. Standardized uptake value. Nuclear medicine and biology 27, 643-646.
IAEA, 2000. Charged-particle cross section database for medical radioisotope production, <https://www-nds.iaea.org/medical/>.
Ido, T., Wan, C.N., Casella, V., Fowler, J.S., Wolf, A.P., Reivich, M., Kuhl, D.E., 1978. Labeled 2-deoxy-D-glucose analogs. 18F-labeled 2-deoxy-2-fluoro-D-glucose, 2-deoxy-2-fluoro-D-mannose and 14C-2-deoxy-2-fluoro-D-glucose. Journal of Labelled Compounds and Radiopharmaceuticals 14, 175-183.
Janssen, M.H., Ollers, M.C., van Stiphout, R.G., Riedl, R.G., van den Bogaard, J., Buijsen, J., Lambin, P., Lammering, G., 2012. PET-based treatment response

evaluation in rectal cancer: prediction and validation. International journal of radiation oncology, biology, physics 82, 871-876.
K. Linga, M., Indrajit, C., 2012. An Introduction to Nuclear Materials: Fundamentals and Applications, First edition ed. Wiley-VCH Verlag GmbH & Co.
Keyes, J.W., Jr., 1995. SUV: standard uptake or silly useless value? Journal of nuclear medicine : official publication, Society of Nuclear Medicine 36, 1836-1839.
Kilbourn, M.R., Jerabek, P.A., Welch, M.J., 1985. An improved [18O]water target for [18F]fluoride production. The International journal of applied radiation and isotopes 36, 327-328.
Kim, C.K., Gupta, N.C., Chandramouli, B., Alavi, A., 1994. Standardized uptake values of FDG: body surface area correction is preferable to body weight correction. Journal of nuclear medicine : official publication, Society of Nuclear Medicine 35, 164-167.
Knowles, S.M., Wu, A.M., 2012. Advances in immuno-positron emission tomography: antibodies for molecular imaging in oncology. Journal of clinical oncology : official journal of the American Society of Clinical Oncology 30, 3884-3892.
Knust, E.J., Machulla, H.J., 1983. High yield production of 18F in a water target via the 16O(3He,p)18F reaction. The International journal of applied radiation and isotopes 34, 1627-1628.
Larsson, E., Ljungberg, M., Strand, S.E., Jonsson, B.A., 2011. Monte Carlo calculations of absorbed doses in tumours using a modified MOBY mouse phantom for pre-clinical dosimetry studies. Acta oncologica (Stockholm, Sweden) 50, 973-980.
Larsson, E., Strand, S.E., Ljungberg, M., Jonsson, B.A., 2007. Mouse S-factors based on Monte Carlo simulations in the anatomical realistic Moby phantom for internal dosimetry. Cancer biotherapy & radiopharmaceuticals 22, 438-442.
Lawrence, E.O., 1934. Radioactive Sodium Produced by Deuton Bombardment. Physical Review 46, 746-746.
Lebeda, O., Jiran, R., Ráliš, J., Štursa, J., 2005. A new internal target system for production of 211At on the cyclotron U-120M. Applied Radiation and Isotopes 63, 49-53.
Ledingham, K.W.D., McKenna, P., McCanny, T., Shimizu, S., Yang, J.M., Robson, L., Zweit, J., Gillies, J.M., Bailey, J., Chimon, G.N., Clarke, R.J., Neely, D., Norreys, P.A., Collier, J.L., Singhal, R.P., Wei, M.S., Mangles, S.P.D., Nilson, P., Krushelnick, K., Zepf, M., 2004. High power laser production of short-lived isotopes for positron emission tomography. Journal of Physics D: Applied Physics 37, 2341.
Lee, K.H., Ko, B.H., Paik, J.Y., Jung, K.H., Choe, Y.S., Choi, Y., Kim, B.T., 2005. Effects of anesthetic agents and fasting duration on 18F-FDG biodistribution and insulin levels in tumor-bearing mice. Journal of nuclear medicine : official publication, Society of Nuclear Medicine 46, 1531-1536.

Lindholm, P., Minn, H., Leskinen-Kallio, S., Bergman, J., Ruotsalainen, U., Joensuu, H., 1993. Influence of the blood glucose concentration on FDG uptake in cancer--a PET study. Journal of nuclear medicine : official publication, Society of Nuclear Medicine 34, 1-6.
Lindner, L., Suèr, T.H.G.A., Brinkman, G.A., Veenboer, J.T., 1973. A dynamic "loop"—target for the incyclotron production of 18F by the 16O (α, d)16F reaction on water. The International journal of applied radiation and isotopes 24, 124-126.
Manickam, V., Brey, R.R., Jenkins, P.A., Christian, P.E., 2009. Measurements of activation products associated with Havar foils from a GE PETtrace medical cyclotron using high resolution gamma spectroscopy. Health physics 96, S37-42.
McCarthy, D.W., Bass, L.A., Cutler, P.D., Shefer, R.E., Klinkowstein, R.E., Herrero, P., Lewis, J.S., Cutler, C.S., Anderson, C.J., Welch, M.J., 1999. High purity production and potential applications of copper-60 and copper-61. Nuclear medicine and biology 26, 351-358.
McCarthy, D.W., Shefer, R.E., Klinkowstein, R.E., Bass, L.A., Margeneau, W.H., Cutler, C.S., Anderson, C.J., Welch, M.J., 1997. Efficient production of high specific activity 64Cu using a biomedical cyclotron. Nuclear medicine and biology 24, 35-43.
Medema, J., Elsinga, P.H., Bruessermann, M., van Essen, J., Paans, A.M.J., 2002. Production of F-18 fluoride in the nuclear interface titanium target on a MC-17 cyclotron, Ninth international workshop on targetry and target chemistry.
Meijs, W.E., Herscheid, J.D.M., Haisma, H.J., Wijbrandts, R., van Langevelde, F., Van Leuffen, P.J., Mooy, R., Pinedo, H.M., 1994. Production of highly pure no-carrier added 89Zr for the labelling of antibodies with a positron emitter. Applied Radiation and Isotopes 45, 1143-1147.
Mustafa, M.G., West, H.I., Jr., O'Brien, H., Lanier, R.G., Benhamou, M., Tamura, T., 1988. Measurements and a direct-reaction-plus-Hauser-Feshbach analysis of 89Y(p,n)89Zr, 89Y(p,2n)88, and 89Y(p,pn)88Y reactions up to 40 MeV. Physical review C: Nuclear physics 38, 1624-1637.
Nickles, R.J., Daube, M.E., Ruth, T.J., 1984. An 18O2 target for the production of [18F]F2. The International journal of applied radiation and isotopes 35, 117-122.
Nickles, R.J., Kulago, A.A., Schueller, M.J., Stone, C.K., 1997. A rather intense source of fast neutrons for small scale activation. Applied radiation and isotopes : including data, instrumentation and methods for use in agriculture, industry and medicine 48, 55-58.
Nozaki, T., Tanaka, Y., Shimamura, A., Karasawa, T., 1968. The preparation of anhydrous HF18. The International journal of applied radiation and isotopes 19, 27-32.
Ohlsson, T., 1996. A clinical positron emission tomography facility, Department of radiation physics, The jubileum institute. Lund University.
Ohlsson, T., Sandell, A., Hellborg, R., Håkansson, K., Nilsson, C., Strand, S.E., 1996. Clinical useful quantities of [18F]fluoride produced by 6 MeV proton irradiation of a H2 18O target. Nuclear Instruments and Methods in Physics

Research Section A: Accelerators, Spectrometers, Detectors and Associated Equipment 379, 341-342.
P. Schaffer, F. Bénard, A. Bernstein, K. Buckley, A. Celler, N. Cockburn, J. Corsaut, M. Dodd, C. Economou, T. Eriksson, M. Frontera, V. Hanemaayer, B. Hook, J. Klug, M. Kovacs, F.S. Prato, S. McDiarmid, T.J. Ruth, C. Shanks, J.F. Valliant, S. Zeisler, U. Zetterberg, P.A. Zavodszky, 2014. Direct Production of 99mTc via 100Mo(p,2n) on Small Medical Cyclotrons, Physics Procedia, 23rd Conference on Application of Accelerators in Research and Industry, 2014, in press.
Pagani, M., Stone-Elander, S., Larsson, S.A., 1997. Alternative positron emission tomography with non-conventional positron emitters: effects of their physical properties on image quality and potential clinical applications. European journal of nuclear medicine 24, 1301-1327.
Patlak, C.S., Blasberg, R.G., Fenstermacher, J.D., 1983. Graphical evaluation of blood-to-brain transfer constants from multiple-time uptake data. Journal of cerebral blood flow and metabolism : official journal of the International Society of Cerebral Blood Flow and Metabolism 3, 1-7.
Phelps, M.E., Hoffman, E.J., Mullani, N.A., Ter-Pogossian, M.M., 1975. Application of Annihilation Coincidence Detection to Transaxial Reconstruction Tomography. Journal of Nuclear Medicine 16, 210-224.
Phelps, M.E., Huang, S.C., Hoffman, E.J., Selin, C., Sokoloff, L., Kuhl, D.E., 1979. Tomographic measurement of local cerebral glucose metabolic rate in humans with (F-18)2-fluoro-2-deoxy-D-glucose: validation of method. Ann Neurol 6, 371-388.
Phelps, M.E., Mazziotta, J.C., Schelbert, H.R., 1986. Positron emission tomography and autoradiography: principles and applications for the brain and heart. Raven Press.
Printz, G., Solin, O., 1991. Construction of an 18O-enriched water target for the routine production of [18O]fluoride. Acta radiologica. Supplementum 376, 59.
Rasbridge, S.A., Gillett, C.E., Seymour, A.M., Patel, K., Richards, M.A., Rubens, R.D., Millis, R.R., 1994. The effects of chemotherapy on morphology, cellular proliferation, apoptosis and oncoprotein expression in primary breast carcinoma. British journal of cancer 70, 335-341.
Reichert, J.M., 2008. Monoclonal antibodies as innovative therapeutics. Current pharmaceutical biotechnology 9, 423-430.
Reichert, J.M., Valge-Archer, V.E., 2007. Development trends for monoclonal antibody cancer therapeutics. Nature reviews. Drug discovery 6, 349-356.
Rhodes, C.G., Wise, R.J., Gibbs, J.M., Frackowiak, R.S., Hatazawa, J., Palmer, A.J., Thomas, D.G., Jones, T., 1983. In vivo disturbance of the oxidative metabolism of glucose in human cerebral gliomas. Ann Neurol 14, 614-626.
Robert Dahl, J., Lee, R., Bigler, R.E., Schmall, B., Aber, J.E., 1983. A new target system for the preparation of no-carrier-added 18F-fluorinating compounds. The International journal of applied radiation and isotopes 34, 693-700.

Rowshanfarzad, P., Sabet, M., Reza Jalilian, A., Kamalidehghan, M., 2006. An overview of copper radionuclides and production of 61Cu by proton irradiation of natZn at a medical cyclotron. Applied Radiation and Isotopes 64, 1563-1573.
Ruth T, J., Wolf A, P., 1979. Absolute Cross Sections for the Production of 18F via the 18O(p, n)18F Reaction, Radiochimca Acta, p. 21.
Saha, J.K., Xia, J., Grondin, J.M., Engle, S.K., Jakubowski, J.A., 2005. Acute hyperglycemia induced by ketamine/xylazine anesthesia in rats: mechanisms and implications for preclinical models. Experimental biology and medicine (Maywood, N.J.) 230, 777-784.
Schmitz, F., Monclus, M., Van Naemen, J., Ekelmans, D., Goldman, S., Verbruggen, R., Vamecq, F., Jongen, Y., Van Langevelde, F., Kruijer, P.S., Van Leuffen, P.J., Mooij, R., Van der Jag, P.J., 2002. Production of Multicurie [18F]Fluoride using a Niobium Target Chamber at small PET cyclotrons, Ninth International Workshop on Targetry and Target Chemistry, Turku, Finland.
Severin, G.W., Engle, J.W., Barnhart, T.E., Nickles, R.J., 2011. 89Zr radiochemistry for positron emission tomography. Medicinal chemistry (Shariqah (United Arab Emirates)) 7, 389-394.
Shiue, C.-Y., Salvadori, P.A., Wolf, A.P., Fowler, J.S., MacGregor, R.R., 1982. A New Improved Synthesis of 2-Deoxy-2-[18F]Fluoro-D-Glucose from 18F-Labeled Acetyl Hypofluorite. Journal of Nuclear Medicine 23, 899-903.
Shure, K., Deutsch, M., 1951. Radiations from zirconium89. Physical Review 82, 122-122.
Siikanen, J., Sandell, A., 2010. A solid 110, 111, 114m-Indium target with online thermal diffusion activity extraction- Work In Progress, The 13th International Workshop on Targetry and Target Chemistry Proceedings. DTU, Risö, Denmark.
Siikanen, J., Valdovinos, H.F., Hernandez, R., Coarasa, A.A., McGoron, A., Sandell, A., Barnhart, T.E., Nickles, R.J., 2013. Cyclotron Produced Ga-66/68 with Thermal Diffusion-Assisted Bulk Separation and AG50W-X8/UTEVA Purification, Radiometals 2013 in Sonoma Valley, Sonoma Valley, CA, USA.
Sloan, D.H., Lawrence, E.O., 1931. The Production of Heavy High Speed Ions without the Use of High Voltages. Physical Review 38, 2021-2032.
Sokoloff, L., Reivich, M., Kennedy, C., Des Rosiers, M.H., Patlak, C.S., Pettigrew, K.D., Sakurada, O., Shinohara, M., 1977. The [14C]deoxyglucose method for the measurement of local cerebral glucose utilization: theory, procedure, and normal values in the conscious and anesthetized albino rat. Journal of neurochemistry 28, 897-916.
Solomayer, E.F., Becker, S., Pergola-Becker, G., Bachmann, R., Krämer, B., Vogel, U., Neubauer, H., Wallwiener, D., Huober, J., Fehm, T.N., 2006. Comparison of HER2 status between primary tumor and disseminated tumor cells in␣primary breast cancer patients. Breast Cancer Res Treat 98, 179-184.
Stabin, M.G., Sparks, R.B., Crowe, E., 2005. OLINDA/EXM: the second-generation personal computer software for internal dose assessment in nuclear medicine. Journal of nuclear medicine : official publication, Society of Nuclear Medicine 46, 1023-1027.

Steinbach, J., Guenther, K., Loesel, E., Grunwald, G., Mikecz, P., Ando, L., Szelecsenyi, F., Beyer, G.J., 1990. Temperature course in small volume [18O]water targets for [18F]F- production. International journal of radiation applications and instrumentation. Part A, Applied radiation and isotopes 41, 753-756.
Steyn, G.F., Vermeulen, C., Botha, A.H., Conradie, J.L., Crafford, J.P.A., Delsink, J.L.G., Dietrich, J., du Plessis, H., Fourie, D.T., Kormány, Z., van Niekerk, M.J., Rohwer, P.F., Stodart, N.P., de Villiers, J.G., 2013. A vertical-beam target station and high-power targetry for the cyclotron production of radionuclides with medium energy protons. Nuclear Instruments and Methods in Physics Research Section A: Accelerators, Spectrometers, Detectors and Associated Equipment 727, 131-144.
Svensson, C., 2008. Production of 89Zr for labelling of antibodies to be evaluated preclinically with micro-PET for radioimmunodiagnostics of prostate cancer. Lund University.
Tahari, A.K., Chien, D., Azadi, J.R., Wahl, R.L., 2014. Optimum lean body formulation for correction of standardized uptake value in PET imaging. Journal of nuclear medicine : official publication, Society of Nuclear Medicine 55, 1481-1484.
Thisgaard, H., Jensen, M., Elema, D.R., 2011. Medium to large scale radioisotope production for targeted radiotherapy using a small PET cyclotron. Applied Radiation and Isotopes 69, 1-7.
Tolmachev, V., Bernhardt, P., Forssell-Aronsson, E., Lundqvist, H., 2000. 114mIn, a candidate for radionuclide therapy: low-energy cyclotron production and labeling of DTPA-D-phe-octreotide. Nuclear medicine and biology 27, 183-188.
Tolmachev, V., Lundqvist, H., 1996. Rapid separation of gallium from zinc targets by thermal diffusion. Applied Radiation and Isotopes 47, 297-299.
Tolmachev, V., Lundqvist, H., Einarsson, L., 1998. Production of 61Cu from a natural nickel target. Applied Radiation and Isotopes 49, 79-81.
Toyama, H., Ichise, M., Liow, J.S., Modell, K.J., Vines, D.C., Esaki, T., Cook, M., Seidel, J., Sokoloff, L., Green, M.V., Innis, R.B., 2004. Absolute quantification of regional cerebral glucose utilization in mice by 18F-FDG small animal PET scanning and 2-14C-DG autoradiography. Journal of nuclear medicine : official publication, Society of Nuclear Medicine 45, 1398-1405.
Wahl, R.L., Henry, C.A., Ethier, S.P., 1992. Serum glucose: effects on tumor and normal tissue accumulation of 2-[F-18]-fluoro-2-deoxy-D-glucose in rodents with mammary carcinoma. Radiology 183, 643-647.
Valdovinos, H.F., Hernandez, R., Barnhart, T.E., Graves, S., Cai, W., Nickles, R.J., 2015. Separation of cyclotron-produced 44Sc from a natural calcium target using a dipentyl pentylphosphonate functionalized extraction resin. Applied Radiation and Isotopes 95, 23-29.

van Dongen, G.A., Vosjan, M.J., 2010. Immuno-positron emission tomography: shedding light on clinical antibody therapy. Cancer biotherapy & radiopharmaceuticals 25, 375-385.
Weber, W.A., 2009. Assessing tumor response to therapy. Journal of nuclear medicine : official publication, Society of Nuclear Medicine 50 Suppl 1, 1S-10S.
Vera Ruiz, H., 1988. Report of an International Atomic Energy Agency's consultants' meeting on fluorine 18: Reactor production and utilization. International Journal of Radiation Applications and Instrumentation. Part A. Applied Radiation and Isotopes 39, 31-39.
Verbraecken, J., Van de Heyning, P., De Backer, W., Van Gaal, L., 2006. Body surface area in normal-weight, overweight, and obese adults. A comparison study. Metabolism: clinical and experimental 55, 515-524.
Verel, I., Visser, G.W.M., Boellaard, R., Stigter-van Walsum, M., Snow, G.B., van Dongen, G.A.M.S., 2003. 89Zr Immuno-PET: Comprehensive Procedures for the Production of 89Zr-Labeled Monoclonal Antibodies. Journal of Nuclear Medicine 44, 1271-1281.
Vereshchagin, Y.I., Zagryadskiy, V.A., Prusakov, V.N., 1993. Cyclotron 82Sr production for medical applications. Nuclear Instruments and Methods in Physics Research Section A: Accelerators, Spectrometers, Detectors and Associated Equipment 334, 246-248.
Western, J., 1991. Mechanical Safety Subcommittee Guideline for Design of thin Windows for Vacuum Vessels, Fermi National Accelerator Laboratory.
Wong, K.P., Sha, W., Zhang, X., Huang, S.C., 2011. Effects of administration route, dietary condition, and blood glucose level on kinetics and uptake of 18F-FDG in mice. Journal of nuclear medicine : official publication, Society of Nuclear Medicine 52, 800-807.
Woo, S.K., Lee, T.S., Kim, K.M., Kim, J.Y., Jung, J.H., Kang, J.H., Cheon, G.J., Choi, C.W., Lim, S.M., 2008. Anesthesia condition for (18)F-FDG imaging of lung metastasis tumors using small animal PET. Nuclear medicine and biology 35, 143-150.
Vosjan, M.J., Perk, L.R., Visser, G.W., Budde, M., Jurek, P., Kiefer, G.E., van Dongen, G.A., 2010. Conjugation and radiolabeling of monoclonal antibodies with zirconium-89 for PET imaging using the bifunctional chelate p-isothiocyanatobenzyl-desferrioxamine. Nature Protocols 5, 739-743.
Vugts, D.J., van Dongen, G.A.M.S., 2011. 89Zr-labeled compounds for PET imaging guided personalized therapy. Drug Discovery Today: Technologies 8, e53-e61.
Zeisler, S.K., Becker, D.W., Pavan, R.A., Moschel, R., Rühle, H., 2000. A water-cooled spherical niobium target for the production of [18F]fluoride. Applied Radiation and Isotopes 53, 449-453.
Zidan, J., Dashkovsky, I., Stayerman, C., Basher, W., Cozacov, C., Hadary, A., 2005. Comparison of HER-2 overexpression in primary breast cancer and metastatic sites and its effect on biological targeting therapy of metastatic disease. Br J Cancer 93, 552-556.

Ziegler, J.F., Ziegler, M.D., Biersack, J.P., 2010. SRIM – The stopping and range of ions in matter (2010). Nuclear Instruments and Methods in Physics Research Section B: Beam Interactions with Materials and Atoms 268, 1818-1823.
Zinzani, P.L., Tani, M., Fanti, S., Alinari, L., Musuraca, G., Marchi, E., Stefoni, V., Castellucci, P., Fina, M., Farshad, M., Pileri, S., Baccarani, M., 2006. Early positron emission tomography (PET) restaging: a predictive final response in Hodgkin's disease patients. Annals of Oncology 17, 1296-1300.
Örbom, A., 2013. Preclinical Molecular Imaging using Multi-Isotope Digital Autoradiography, Department of Medical Radiation Physics. Lund University.